SCIENTIFIC REPORTS

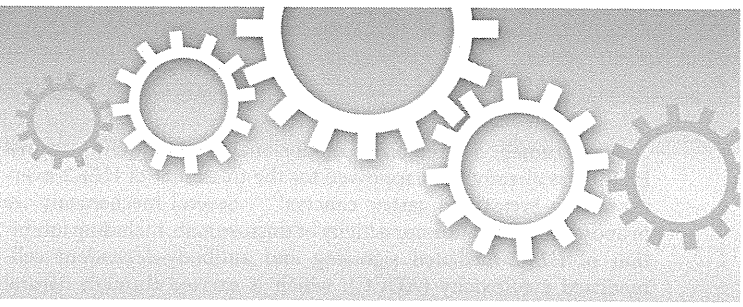

OPEN

SUBJECT AREAS:
TARGETED THERAPIES
CANCER IMMUNOTHERAPY
TRANSLATIONAL RESEARCH
SMALL-CELL LUNG CANCER

Received
17 June 2013

Accepted
30 August 2013

Published
16 September 2013

Correspondence and requests for materials should be addressed to T.K. (tkijima@imed3.med.osaka-u.ac.jp)

Overcoming chemoresistance of small-cell lung cancer through stepwise HER2-targeted antibody-dependent cell-mediated cytotoxicity and VEGF-targeted antiangiogenesis

Toshiyuki Minami[1], Takashi Kijima[1], Satoshi Kohmo[1], Hisashi Arase[2,3], Yasushi Otani[1], Izumi Nagatomo[1], Ryo Takahashi[1], Kotaro Miyake[1], Masayoshi Higashiguchi[1], Osamu Morimura[1], Shoichi Ihara[1], Kazuyuki Tsujino[1], Haruhiko Hirata[1], Koji Inoue[1], Yoshito Takeda[1], Hiroshi Kida[1], Isao Tachibana[1] & Atsushi Kumanogoh[1,3,4]

[1]Department of Respiratory Medicine, Allergy and Rheumatic Diseases, Osaka University Graduate School of Medicine, Osaka, Japan, [2]Laboratory of Immunochemistry, World Premier International Research Center (WPI), Immunology Frontier Research Center, and Department of Immunochemistry, Research Institute for Microbial Disease, Osaka University, Suita, Osaka, Japan, [3]Core Research for Evolutional Science and Technology, Japan Science and Technology Agency, 4-1-8, Honcho Kawaguchi, Saitama 332-0012, Japan, [4]Department of Immunopathology, Immunology Frontier Research Center, Osaka University, Osaka, Japan.

Small-cell lung cancer (SCLC) easily recurs with a multidrug resistant phenotype. However, standard therapeutic strategies for relapsed SCLC remain unestablished. We found that human epidermal growth factor receptor 2 (HER2) is not only expressed in pretreated human SCLC specimens, but is also upregulated when HER2-positive SCLC cells acquire chemoresistance. Trastuzumab induced differential levels of antibody-dependent cell-mediated cytotoxicity (ADCC) to HER2-positive SCLC cells. Furthermore, as a mechanism of the differential levels of ADCC, we have revealed that coexpression of intracellular adhesion molecule (ICAM)-1 on SCLC cells is essential to facilitate and accelerate the trastuzumab-mediated ADCC. Although SN-38–resistant SCLC cells lacking ICAM-1 expression were still refractory to trastuzumab, their *in vivo* growth was significantly suppressed by bevacizumab treatment due to dependence on their distinctive and abundant production of vascular endothelial growth factor. Collectively, stepwise treatment with trastuzumab and bevacizumab is promising for the treatment of chemoresistant SCLC.

Small-cell lung cancer (SCLC) accounts for approximately 15% of primary lung carcinomas and has the poorest outcome of all its histological types. The extreme aggressiveness of SCLC is due to its rapid doubling time, widespread metastases, and development of multidrug resistance (MDR) to chemotherapy[1,2]. The current front-line standard chemotherapy regimen for SCLC, cisplatin plus either etoposide or irinotecan, is effective in most SCLC cases, but the disease recurs with an MDR phenotype shortly after the initial treatment. In addition, there are currently no beneficial standard therapeutic strategies against the recurrent cancer[2–4]. Therefore, there is an urgent need to develop a novel strategy that overcomes MDR and confers significant survival benefits for patients. Although several clinical trials targeting receptor tyrosine kinases (RTKs) have been conducted for recurrent SCLC, they have yielded disappointing results[5,6]. The reasons for this inefficacy are that they are not the RTKs to which SCLC cells are dependent upon for their proliferation, and oncogenic driver mutations have not yet been found in SCLC[7].

Human epidermal growth factor receptor 2 (HER2) belongs to the HER family of RTKs. HER2 can transduce cellular proliferative and survival signals either as a homodimer without ligand-stimulation or a heterodimer with other HER family members upon ligand stimulation[8]. HER2 is overexpressed in about 30% of breast cancers and its overexpression correlates with a poor outcome[9,10]. Similarly, HER2 expression is also an independent negative prognostic factor of extensive disease (ED)-SCLC[11,12].

Trastuzumab, a humanized monoclonal antibody (Ab) against HER2, has already been approved for the treatment of HER2-overexpressing breast and gastric cancers[13,14]. Several mechanisms are proposed for the antitumor activity of trastuzumab, including inhibition of HER2-mediated signaling and antibody-dependent cell-mediated cytotoxicity (ADCC), which is exerted through natural killer (NK) cell–initiated cancer cell lysis[15,16]. SCLC cells have been shown to be generally susceptible to NK cell–mediated lysis[17]. Moreover, chemoresistant SCLC cells exhibit increased susceptibility to lymphokine-activated killer cells compared to their chemosensitive counterparts[18]. Based on these observations, we presumed that HER2 is targetable by trastuzumab especially in chemoresistant HER2-positive SCLC.

We here investigated the therapeutic potential and mechanisms of trastuzumab toward HER2-positive MDR SCLC. Furthermore, we evaluated the salvage therapeutic efficacy of bevacizumab, a humanized monoclonal Ab against vascular endothelial growth factor (VEGF), on trastuzumab-refractory SCLC.

Results

Establishment of a highly sensitive immunohistochemistry (IHC) system to detect HER2 in SCLC. Since HER2 expression is upregulated in chemoresistant SCLC cells[19], it is reasonable to target HER2 in SCLC patients who have become resistant to the front-line chemotherapy. HercepTest is commonly used to select eligible patients for trastuzumab therapy in breast and gastric cancer[14,20,21]. We first performed HercepTest using formalin-fixed paraffin-embedded blocks of SK-BR-3 (positive control, breast cancer cell line), H69 (negative control), SBC-3, and etoposide-resistant SBC-3/ETP cells. HER2 was strongly stained in SK-BR-3 cells, but not in parental SBC-3 cells and was faintly detected even in HER2-upregulated SBC-3/ETP cells (Figure 1a). These results led us to establish a new IHC detection system with higher sensitivity applicable to SCLC.

We performed the antigen retrieval step under higher alkaline conditions at pH 9.0, compared to the generally approved pH 6.0, to enhance the detection of cell surface membrane proteins. We also used a rabbit anti-human HER2 monoclonal Ab (clone D8F12) as the detection antibody. These two IHC methodological modifications succeeded in detecting HER2 in SBC-3 and SBC-3/ETP cells, while H69 cells remained HER2-negative, indicating that these modifications increased the sensitivity without compromising the specificity of the assay (Figure 1a). Moreover, we confirmed that this IHC system could also detect HER2 in human SCLC biopsy samples (Figure 1b). Of 10 samples obtained from individual patients, three were HER2-positive (Figure 1b and Supplementary Figure 1a and b), whereas nine were not stained at all shown as the representative two cases (Figure 1b) and only one specimen was faintly stained by HercepTest. Therefore, all cases were considered HER2-negative by HercepTest scoring system[21].

Effect of trastuzumab monotherapy against HER2-positive SCLC cells. To confirm whether trastuzumab can directly bind to cell surface HER2 on SCLC cells, we performed fluorescence-activated cell sorting (FACS) analysis using trastuzumab as the primary antibody. Trastuzumab recognized HER2 in six of 10 SCLC cell lines of Japanese origin but in none of three cell lines of Caucasian origin (Supplementary Figure 2a), suggesting the existence of ethnic difference about HER2 expression in SCLC. Moreover, it also detected HER2 upregulation in various types of chemoresistant SBC-3 sublines regardless of the differential resistant mechanisms (Supplementary Figure 2b).

We next investigated whether trastuzumab monotherapy could inhibit proliferation of HER2-positive SCLC cells. Various concentrations of either trastuzumab or human normal IgG ranging from 0 to 100 μg/ml were added to cultures of HER2-positive SCLC and breast cancer cells, and the antiproliferative effects were assessed by

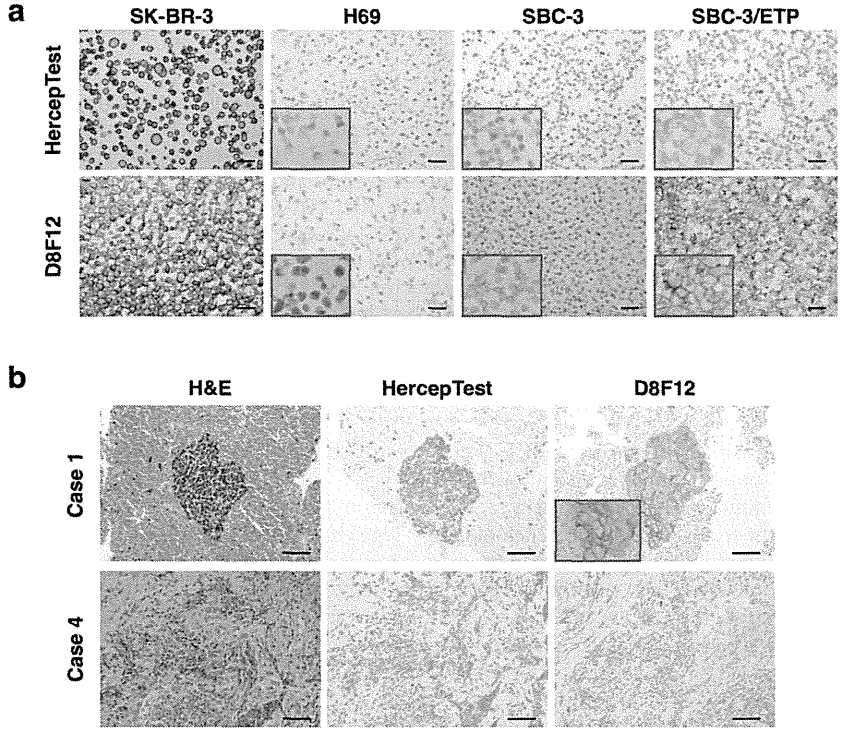

Figure 1 | Development of a highly sensitive IHC system to detect HER2 in SCLC. (a) Detection of HER2 by IHC in breast cancer (SK-BR-3) and SCLC (H69, SBC-3, and SBC-3/ETP) cell blocks by HercepTest (top panels) or the new system (bottom panels). SK-BR-3 and H69 cells were used as a positive and negative control, respectively. The D8F12 Ab-based new IHC system exhibited improved sensitivity compared with HercepTest without compromising specificity. (b) The new IHC system also works well in human SCLC samples obtained by diagnostic biopsy. Representative histological images of HER2-positive (top panels) and -negative (bottom panels) cases are shown. All scale bars, 50 μm.

CCK-8, a tetrazolium reagent, assay. More than 1 μg/ml of trastuzumab significantly inhibited the proliferation of HER2-overexpressing SK-BR-3 cells but had no effect on HER2-positive SCLC cells (Figure 2a).

We then examined how trastuzumab affects HER2-mediated downstream signaling by comparing SBC-3/ETP cells with SK-BR-3 cells. Exposure to 10 μg/ml of trastuzumab increased the levels of phosphorylated HER2 in both SBC-3/ETP and SK-BR-3 cells for up to 6 h. However, the phosphorylation levels returned to basal levels after 24 h in both cell lines. Phosphorylations of Akt and extracellular signal–regulated kinase (Erk) 1/2 were remarkably decreased in SK-BR-3 cells from 3 to 72 h after trastuzumab exposure, whereas they were not affected throughout the 72-h treatment in SBC-3/ETP cells. Cleavage of poly (ADP-ribose) polymerase (PARP) was not observed in either cell line (Figure 2b). These results indicate that trastuzumab transiently upregulates the phosphorylation status of HER2 but does not affect the downstream mitogen-activated protein kinase and Akt pathways in SBC-3/ETP cells. This may explain why trastuzumab did not inhibit the proliferation of HER2-positive SCLC cells.

Trastuzumab-mediated ADCC against HER2-positive SCLC cells. ADCC, as opposed to direct HER2-signaling inhibition, has been proposed as the major antitumor mechanism for trastuzumab[15,16]. We then tested whether trastuzumab could mediate ADCC against HER2-positive SCLC cells by coincubation assay with NK cells. We utilized 3 NK cell lines, YTS, NKL, and NK92MI. Before performing the ADCC assay, we examined the expression levels of Fcγ receptor III (CD16) on each NK cell line because this receptor is indispensable for ADCC. After 4-h exposure to trastuzumab, FACS analysis revealed that CD16 expression was upregulated in YTS and NKL cells but not in NK92MI cells (Figure 2c). Trastuzumab exerted various degrees of killing against HER2-positive SCLC and SK-BR-3 cells when cocultured with YTS or NKL cells. Notably, SBC-3/ETP cells were the most susceptible among the HER2-positive SCLC cells (Figure 2d and e). However, trastuzumab-mediated killing was not induced by NK92MI cells (Figure 2f). These results suggest that HER2-positive SCLC cells were lysed by trastuzumab-mediated ADCC.

Antitumor effects of trastuzumab upon HER2-positive SCLC tumor xenografts. We next investigated the antitumor efficacy of trastuzumab in nude mice bearing HER2-positive SCLC xenografts. As shown in Figure 3a, intraperitoneal injection of 30 mg/kg of trastuzumab twice weekly significantly inhibited the growth of cisplatin-resistant SBC-3/CDDP and SBC-3/ETP but not irinotecan-resistant SBC-3/SN-38 subcutaneous tumors in mice ($P = 0.042$ in SBC-3/CDDP xenografts and $P < 0.001$ in SBC-3/ETP xenografts). These results were consistent with the *in vitro* ADCC assays. Especially, tumor growth was inhibited in all of the seven trastuzumab-treated SBC-3/ETP tumor-bearing mice, two of which achieved complete remission. Additionaly, same tendency was confirmed at a lower dose administration of trastuzumab (10 mg/kg, twice weekly) (Supplementary Figure 3). Furthermore, in SBC-3/ETP xenografts, terminal deoxynucleotidyl transferase dUTP nick end labeling (TUNEL) staining showed that trastuzumab significantly induced apoptosis of SCLC cells (apoptosis index was 6.20 ± 1.63% in trastuzumab group *vs.* 2.10 ± 0.97% in control group, $P = 0.003$), despite the downregulation of cell surface HER2 expression upon trastuzumab treatment (Figure 3b and c). In addition, CD11b-positive tumor-infiltrating NK cells, macrophages, and granulocytes were significantly recruited into tumor foci upon trastuzumab treatment (25.3 ± 4.2% *vs.* 14.8 ± 2.6%, $P = 0.003$) (Figure 3b and d). By contrast, there was no significant increase in TUNEL- and CD11b-positive cells in SBC-3 xenografts upon trastuzumab treatment (Supplementary Figure 4a–c). These findings suggest that the *in vivo* antitumor effects of trastuzumab are accompanied by tumor-infiltrating ADCC-inducible CD11b-positive immune cells such as NK cells, macrophages and granulocyte.

Internalization, ubuiquitination and lysosomal degradation of trastuzumab. To determine whether the difference of *in vivo* antitumor effects among xenografts depended on the difference of cell surface detention time and/or degradation time of trastuzumab-HER2 complexes, we performed internalization, ubuiquitination and lysosomal degradation assays. Unexpectedly, in all HER2-positive SCLC cells, the cell surface-binding trastuzumab diminished with time during the 37°C incubation, while most trastuzumab remained on cell surface at 4°C (Figure 4a). Moreover, HER2 ubiquitination had already started after 15 min of trastuzumab treatment (Figure 4b). Immunofluorescence studies also showed that most trastuzumab was internalized from the cell surface, colocalized with lysosomes, and underwent clustering after 120 min at 37°C (Figure 4c). From these observations, trastuzumab is internalized shortly after binding to HER2, subsequently undergoes ubiquitinqtion and lysosomal lysis. Therefore, we presumed that trastuzumab-mediated ADCC must occur rapidly after HER2 recognition.

Intracellular adhesion molecule (ICAM)-1 as a facilitator and accelerator of trastuzumab-mediated ADCC. As a strong facilitator and accelerator of rapid ADCC completion, we considered the involvement of cell adhesion molecule to be crucial. Since all of the NK cells used as effectors in ADCC assay abundantly express lymphocyte function–associated antigen (LFA)-1, a heterodimer of CD11a and CD18 (Supplementary Figure 5), we evaluated the expression of its counter receptor, ICAM-1, on target SCLC cells. FACS and IHC analyses showed that ICAM-1 expression was remarkably upregulated in SBC-3/ETP cells compared to parental SBC-3 cells (Figure 5a and b). The same tendency was observed in other etoposide-resistant and parental SCLC cells (H69/VP and H69 cells) (Supplementary Figure 6). A population of chemonaïve SCLC cells in biopsy specimens was also positive for ICAM-1, although the expression pattern was heterogeneous (Figure 5c). Moreover, trastuzumab-mediated ADCC in SBC-3/ETP cells was significantly weakened in the presence of an ICAM-1–blocking antibody (Figure 5d). These results confirmed that trastuzumab-mediated ADCC is augmented by cell surface ICAM-1 expression in target SCLC cells. The supposed role of ICAM-1 involved in the mechanisms of trastuzumab-mediated ADCC is schematized in Figure 5e.

Antitumor activity of bevacizumab against trastuzumab-refractory SBC-3/SN-38 xenografts. In order to establish a novel therapeutic strategy for chemoresistant SCLC, another major problem must be solved. Trastuzumab did not show any antitumor effects against SBC-3/SN-38 cells and xenografts (Figure 2d, e and Figure 3a). Although the *in vitro* proliferation rate of SBC-3/SN-38 cells was the same as the parental and other chemoresistant SBC-3 cells (Figure 6a), the *in vivo* growth rate of SBC-3/SN-38 subcutaneous tumors was much greater than other tumors, regardless of trastuzumab treatment (Figure 3a). Lack of ICAM-1 expression may be essential for intrinsic trastuzumab resistance (Figure 4a). Moreover, the rapid growth rate could also explain the resistance. To address this issue, we focused on the discrepancy between the *in vitro* and *in vivo* growth rates. We found that SBC-3/SN-38 cells distinctively produce considerable amounts of VEGF (Figure 6b and c). Since irinotecan is another key drug for SCLC treatment[3], it is essential to control the growth of SBC-3/SN-38 xenografts for the total treatment of chemoresistant SCLC. Treatment with bevacizumab significantly suppressed the growth of subcutaneous SBC-3/SN-38 tumors in all of seven mice (Figure 6d) with a significant decrease in microvessel density (MVD) and Ki67-positive proliferating cells (Figure 6e–g). On the other hand, bevacizumab treatment could not suppress the growth of SBC-3/ETP xenografts

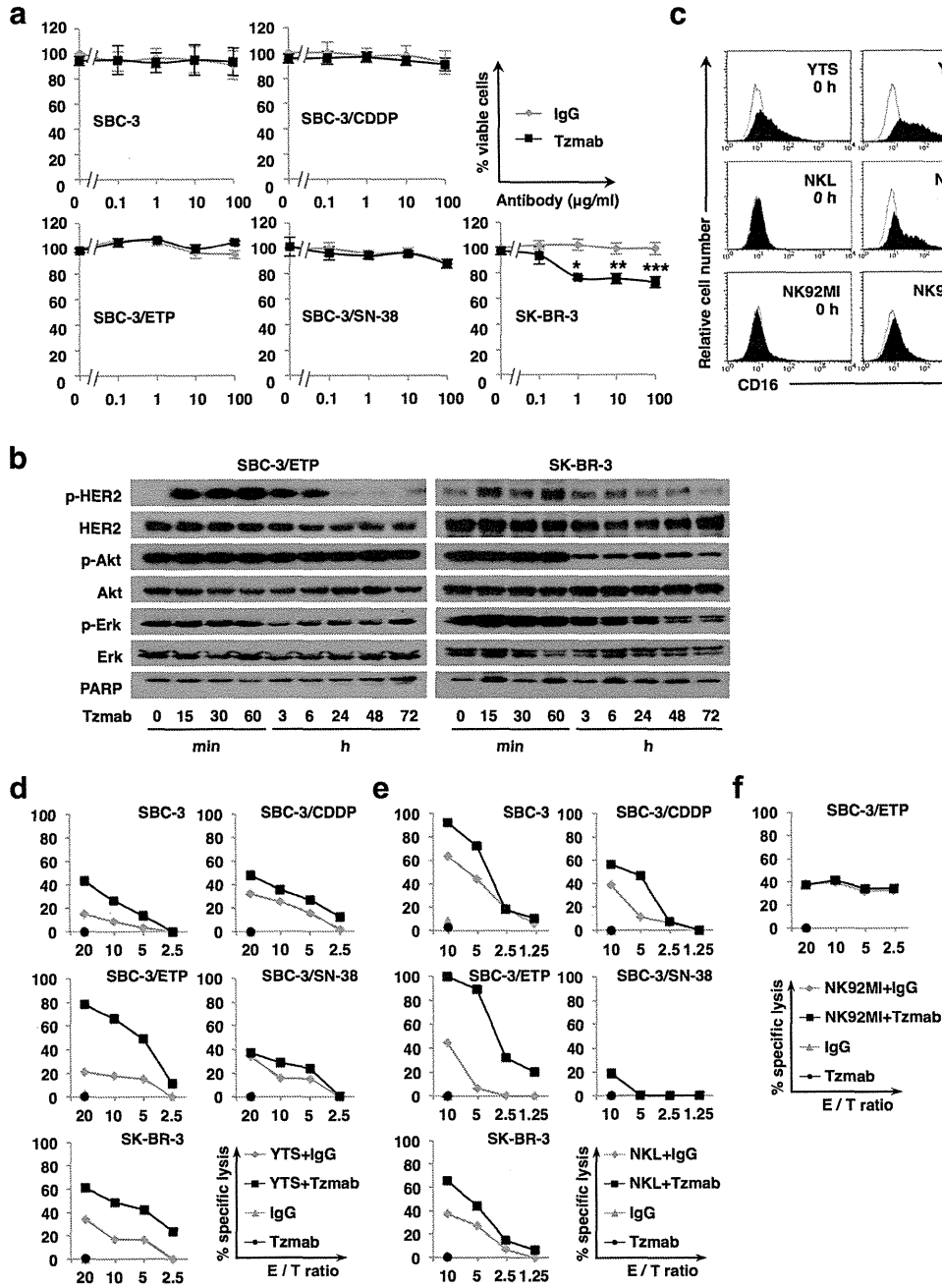

Figure 2 | Antitumor activity of trastuzumab does not depend on direct inhibition of HER2 signaling but rather on ADCC in HER2-positive SCLC cells. (a) HER2-positive SCLC cells (SBC-3, SBC-3/CDDP, SBC-3/ETP, and SBC-3/SN-38 cells) and HER2-overexpressing breast carcinoma cells (SK-BR-3 cells) were treated with 10 μg/ml of normal human IgG or trastuzumab (Tzmab) for 72 h. The relative numbers of viable cells were quantified using the CCK-8 assay. Points, mean% viable cells; bars, SD of at least three independent experiments performed in triplicate; *, $P = 0.018$; **, $P = 0.004$; ***, $P = 0.002$. (b) SBC-3/ETP and SK-BR-3 cells were treated with 10 μg/ml of trastuzumab for up to 72 h. Phosphorylation and expression of HER2, Akt, and Erk in whole cell lysates were examined by immunoblotting. PARP was also examined to detect apoptosis. Each lane of SBC-3/ETP and SK-BR-3 cell lysates contains 60 μg and 30 μg of total protein, respectively. Representative blots from three independent experiments with similar results are shown. Blots are cropped in the figure and full-length blots are presented in Supplementary information. (c) Induction of CD16 expression on NK cells. NK cells (YTS, NKL, and NK92MI cells) were treated with or without 10 μg/ml of trastuzumab for 4 h. Then, the cells were labeled with an anti-CD16 monoclonal Ab (black shaded) or isotype-matched control (solid line) and analyzed for cell surface expression of CD16 by FACS. (d), (e), and (f) Evaluation of trastuzumab-mediated ADCC. Target cancer cells and effector NK cells were coincubated at various E/T ratios with 10 μg/ml of normal human IgG or trastuzumab (Tzmab) for 4 h. Cytotoxic activity was determined based on the LDH release assay. Representative data from at least three experiments are shown as the means of triplicate cultures.

(Supplementary Figure 7), which was likely due to the lack of detectable VEGF production from SBC-3/ETP cells (Figure 6b and c). These results suggest that the antitumor activity of bevacizumab against SBC-3/SN-38 cells depends primarily on the quantity of VEGF produced from tumor cells.

Discussion

We have shown that the immunomodulatory effects of trastuzumab and antiangiogenic effects of bevacizumab are complementary and can provide a novel therapeutic strategy for HER2-expressing chemoresistant SCLC. The antitumor activity of trastuzumab against HER2-positive MDR SCLC occurs mainly through trastuzumab-mediated ADCC but not through its direct inhibition of HER2 signaling. We also revealed that ICAM-1 and HER2 coexpression on target SCLC cells is indispensable to augment trastuzumab-mediated ADCC. Furthermore, we showed that bevacizumab could salvage trastuzumab-resistance through its antiangiogenic effects.

To date, no molecular targeting therapy has been approved for SCLC, because there are no clinical trials that proved significant clinical benefits[5,6]. Although trastuzumab has also been viewed as a promising targeting agent for HER2-positive SCLC[7,22], there has been no preclinical or clinical reports of trastuzumab-based therapy for SCLC. First screening by IHC is useful and crucial for the accurate selection of patients with HER2-targetable SCLC. However, SBC-3 and SBC-3/ETP cells were not or only minimally stained with HercepTest, and were therefore considered negative (Figure 1a and b), although they were HER2-positive by FACS analysis (Supplementary Figure 2b). Moreover, the decision criteria for HER2-positivity with HercepTest differ between gastric and breast cancers[14,20,23]. These observations imply that many false-negative cases would arise

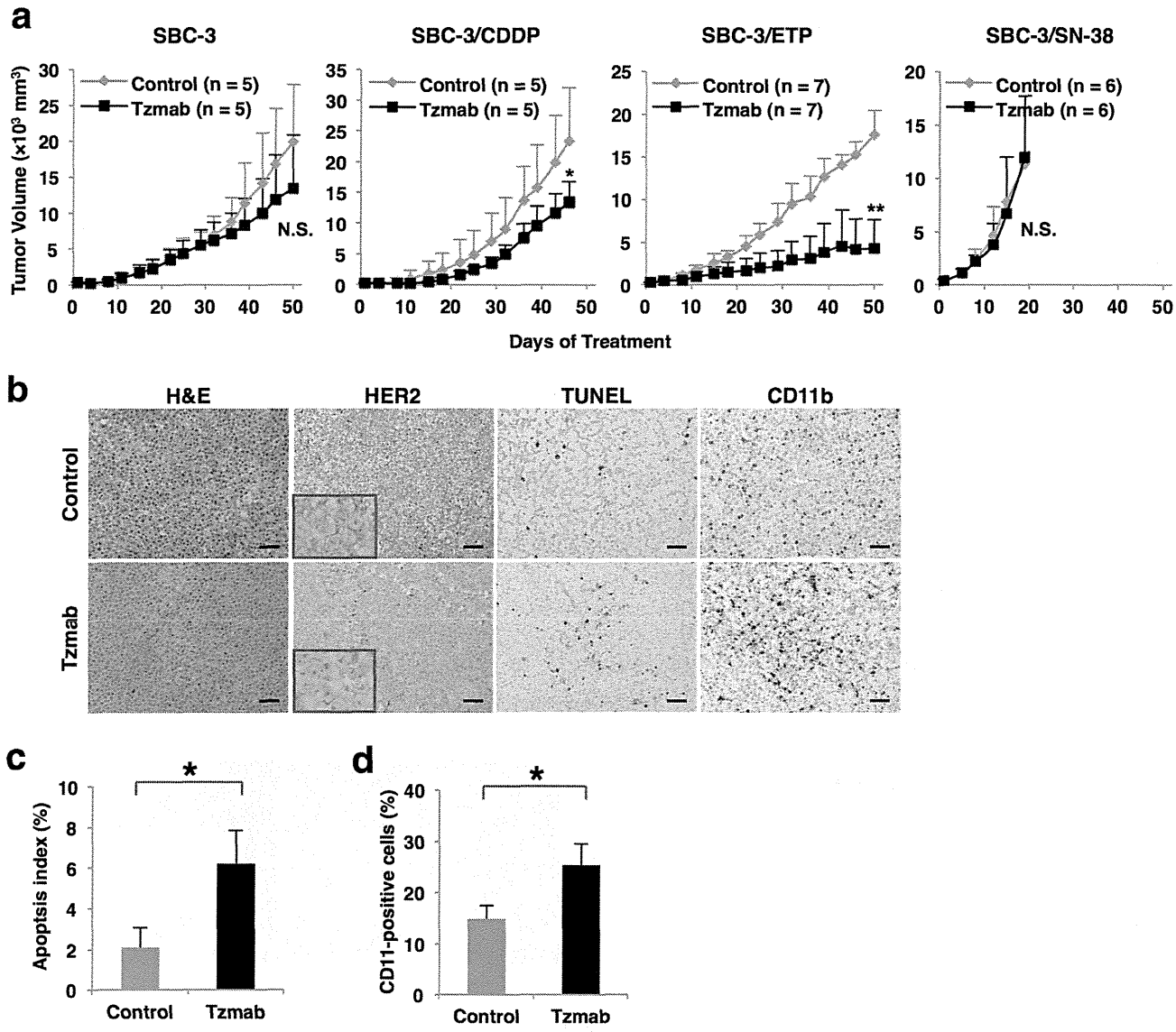

Figure 3 | Antitumor effects of trastuzumab on HER2-positive SCLC tumor xenografts. (a) HER2-positive SCLC cells were inoculated subcutaneously into the flanks of athymic nude mice. When the tumor volume reached approximately 200–300 mm^3, the mice were randomly assigned to the control (PBS) arm or trastuzumab (Tzmab) treatment arm (n = 5–7 mice per group). Trastuzumab was intraperitoneally administered at a dose of 30 mg/kg twice weekly. Points, mean tumor volumes; bars, SD; *, $P = 0.042$; **, $P < 0.001$. (b) Representative histological images of H&E and IHC for HER2, TUNEL, and CD11b. Scale bar, 50 μm. (c) Apoptosis index (%) was determined by calculating the number of TUNEL-positive cells per total number of cells, which consisted of 1000 or more SCLC cells in five randomly selected fields. *, $P = 0.003$. (d) CD11b-positive cells were quantified by counting at least 1000 cells in five randomly selected fields. *, $P = 0.003$.

when HercepTest is used to screen SCLC. To address this issue, we established a new IHC technique with higher sensitivity and comparable specificity to HercepTest (Figure 1a and b). Using this IHC method, we identified three HER2-positive cases out of 10 SCLC biopsy specimens.

Regarding the antitumor mechanism of trastuzumab, Clynes et al. clearly demonstrated the importance of ADCC. They showed that much of the antitumor effects of trastuzumab were lost in mice lacking Fcγ receptor[16]. Actually, HER2-positive SCLC cells were lysed by trastuzumab-mediated ADCC (Figure 2d and e), although their proliferation was not inhibited through suppressing HER2 signal transduction (Figure 2a and b). Also *in vivo*, antitumor effects of trastuzumab were considered to be accompanied by tumor-infiltrating immune cells which could induce ADCC (Figure 3a–d).

Notably, the strength of trastuzumab-mediated ADCC activity was not necessarily proportionate to HER2 expression level (Figure 2d and e, Figure 3a, and Supplementary Figure 2b). This phenomenon has also been observed in clinical trials examining the efficacy of trastuzumab for breast cancer. Namely, more than half of patients with HER2 overexpression showed primary resistance[24,25], whereas some patients with normal HER2 expression benefited from trastuzumab[26]. These observations suggest that HER2 expression is not the only predictor of trastuzumab efficacy. Moreover, trastuzumab-mediated ADCC must occur rapidly after HER2 recognition because trastuzumab was internalized and diminished from cell surface shortly after binding to HER2 (Figure 4a–c). Another cell surface molecule is thought to cooperate with HER2 to facilitate and accelerate the completion of trastuzumab-mediated ADCC.

Engagement of LFA-1 by ICAM-1 promotes strong adhesion between effector and target cells[27], induces polarization of cytolytic granules in NK cells[28], and costimulates the degranulation of NK cells upon antibody-mediated ligation of CD16 with specific antigen on target cells[29,30]. Indeed, SBC-3/ETP (HER2 intermediate/ICAM-1 high) cells were more sensitive than SK-BR-3 (HER2 high/ICAM-1 low) cells to trastuzumab-mediated ADCC (Figure 2d and e, Figure 5a and b, Supplementary Figure 2a and b, and Supplementary Figure 8a and b), and the ADCC activity was canceled by blocking ICAM-1 (Figure 5d). These findings could partly explain why HER2 expression level alone cannot predict the antitumor activity of trastuzumab and imply that ICAM-1 coexpression on target cells is essential for the rapid completion of strong ADCC (Figure 5e).

Since ICAM-1 expression is upregulated when SCLC cells acquire resistance to etoposide (Figure 5a and b, and Supplementary Figure 6), patients with HER2-positive and etoposide-resistant SCLC are ideal candidates for trastuzumab-based therapy. Therefore, future clinical applications of trastuzumab for SCLC should consider combining an initial screening for HER2-positive cases using our highly sensitive IHC method with a secondary screening for ICAM-1–positive cases. Moreover, second-look biopsy is probably more informative to confirm whether HER2 and ICAM-1 expressions are upregulated or homogeneous after acquisition of chemoresistance.

In addition to lack of ICAM-1 expression, upregulation of VEGF production from SCLC cells may be another cause for trastuzumab-resistance. We showed that irinotecan-resistant SCLC cells acquired the potential to produce abundant VEGF (Figure 6b and c). Bevacizumab could salvage irinotecan-resistance by inhibiting VEGF produced from tumor cells (Figure 6d). The efficacy of bevacizumab in combination with cytotoxic drugs in previously untreated SCLC was recently investigated[31,32]. In these studies, bevacizumab combination therapy improved response rate and progression-free survival, but failed to improve overall survival. However, based on our findings, bevacizumab could be an attractive agent

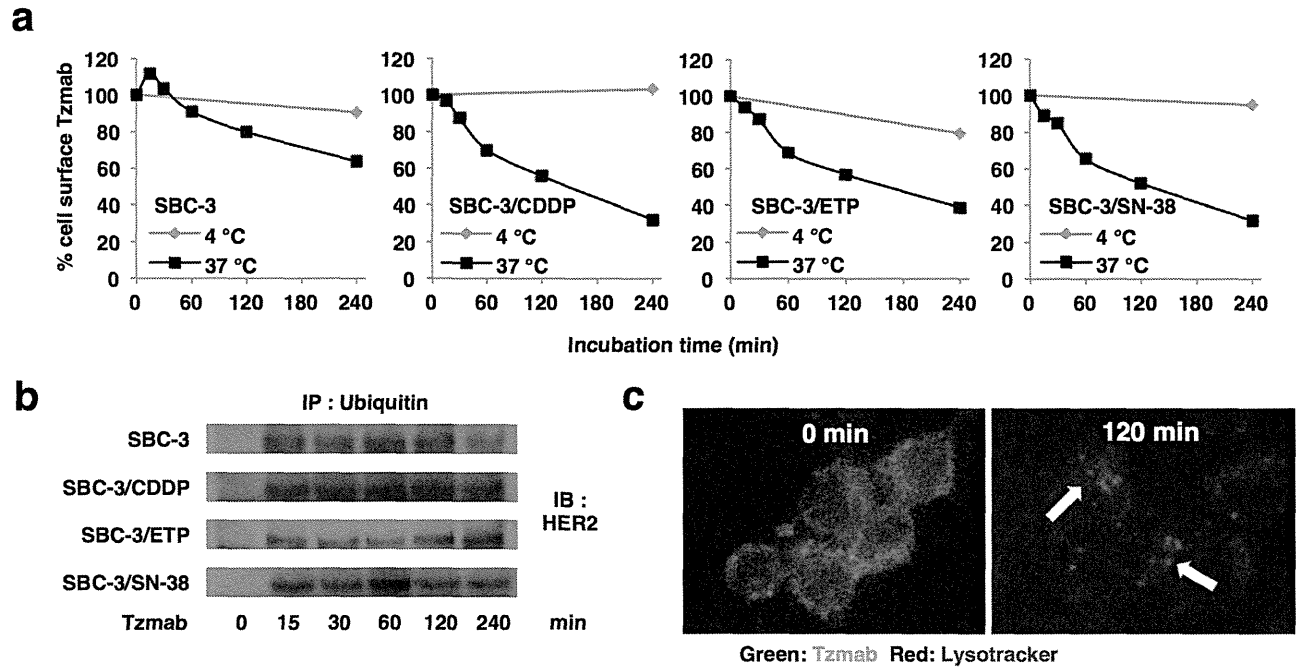

Figure 4 | Trastuzumab is rapidly internalized, and subsequently undergoes ubiquitination and lysosomal degradation. (a) After HER2-positive SCLC cells were incubated with 10 μg/ml of trastuzumab for 45 min at 4°C, cells were warmed to 37°C to allow internalization or maintained at 4°C. The residual levels of cell surface trastuzumab were calculated based on the mean fluorescence intensity (MFI) analyzed by FACSort. (b) After HER2-positive SCLC cells were treated with 10 μg/ml of trastuzumab (Tzmab) for up to 240 min, whole cell lysates were immunoprecipitated with an Ab against ubiquitin. The immunoprecipitant was immunoblotted using an Ab against HER2 to detect HER2 ubiquitination. Blots are cropped in the figure and full-length blots are presented in Supplementary information. (c) SBC-3/CDDP cells were treated with 10 μg/ml of Alexa 488–labeled trastuzumab (green) in the presence of LysoTracker for 45 min at 4°C. Thereafter, trastuzumab was allowed to internalize for up to 120 min at 37°C and fluorescence images are shown. Arrows, lysosomal localization of trastuzumab.

when administered to patients not in front-line but in relapsed stage especially after irinotecan-containing regimens, where its target VEGF exists abundantly.

Finally, we propose a new stepwise approach for SCLC treatment (Figure 7). This new therapeutic approach focusing on MDR relapsed-SCLC for which clinically beneficial standard therapy has not been established is promising to improve the prognosis of SCLC[4]. Patients with HER2-positive SCLC should be selected prior to front-line chemotherapy. When they become resistant to front-line platinum plus either etoposide or irinotecan, trastuzumab- or bevacizumab-containing regimen should be recommended as the second-line therapy, respectively. If these patients acquire further resistance to all of the pretreated drugs, combination of lapatinib, a dual tyrosine kinase inhibitor of EGFR and HER2, and cytotoxic agents could be considered because lapatinib reverses ATP-binding cassette transporter-mediated chemoresistance in SCLC[19]. Alternative therapy with amrubicin, another optional cytotoxic drug for relapsed SCLC, plus either bevacizumab or trastuzumab may also be beneficial to patients who are naïve to either agent.

Recently, the antibody-cytotoxic drug conjugate T-DM1, composed of trastuzumab and emtansine (DM1), was developed and shown to overcome trastuzumab and lapatinib resistance in heavily pretreated HER2-positive metastatic breast cancers[33]. T-DM1 forms a complex with HER2 and undergoes internalization followed by lysosomal degradation. This process results in an intracellular release of DM1 that exerts cytotoxic activity[34]. Moreover, T-DM1 retains all the mechanisms of action of trastuzumab including ADCC[35]. Trastuzumab is rapidly internalized and undergoes lysosomal degradation in SCLC (Figure 4a–c). Although rapid internalization and lysosomal degradation of T-DM1 is disadvantageous for ADCC induction, this process is beneficial because it exerts strong cytotoxic effects in target cells. In this sense, T-DM1 is expected to show antitumor activity even for patients who did not exhibit trastuzumab-mediated ADCC. Thus, T-DM1 is another attractive therapeutic option for HER2-positive MDR SCLC. Collectively, immunomodulation by trastuzumab and antiangiogenesis by bevacizumab are promising strategies for the treatment of chemoresistant SCLC and might have potential to improve the survival of SCLC patients.

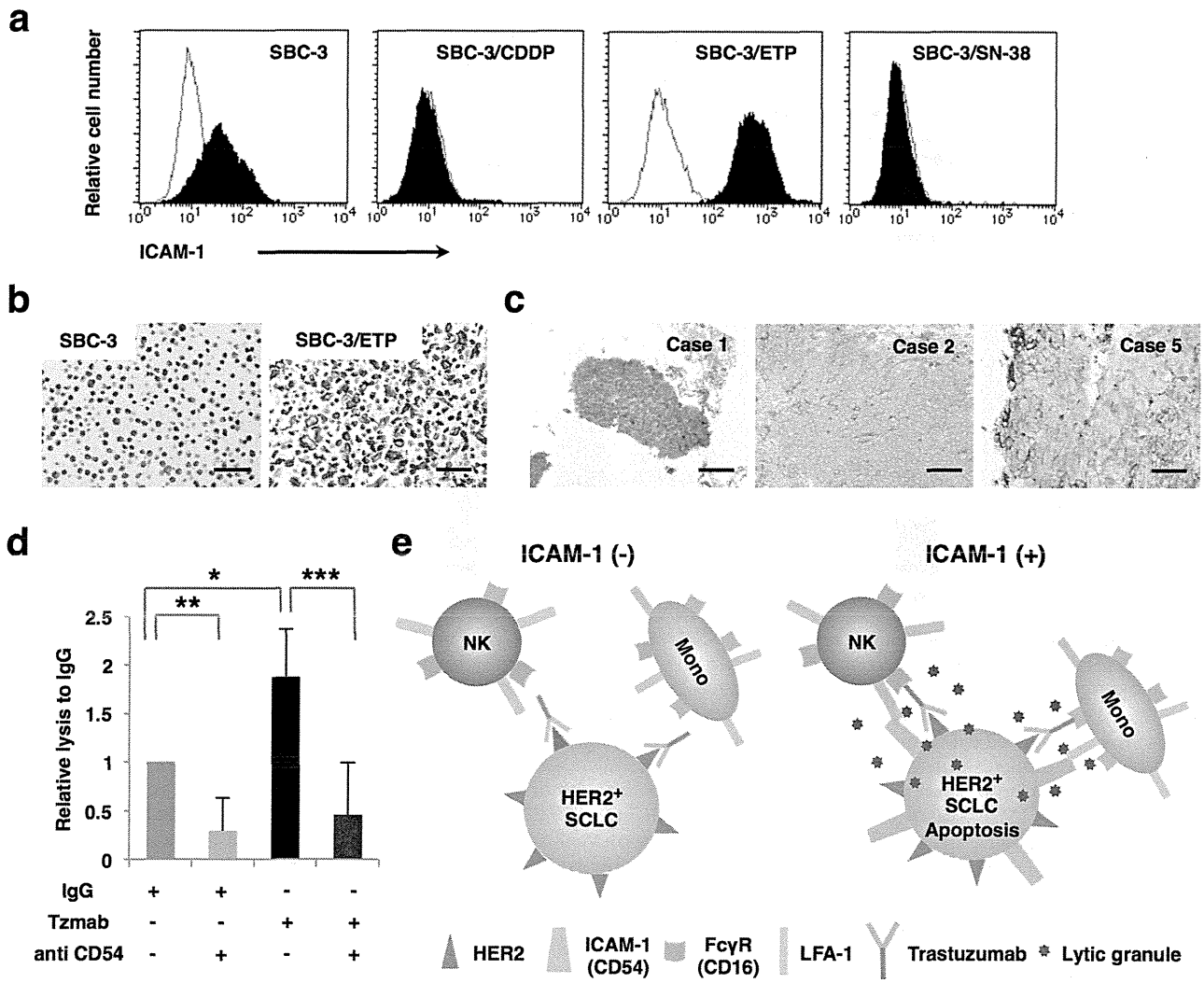

Figure 5 | CAM-1 facilitates trastuzumab-mediated ADCC. (a) Parental and chemoresistant SBC-3 cells are labeled with 5 μg/ml of either an anti-CD54 mouse monoclonal Ab (black shaded) or an isotype-matched control Ab (solid line) and presented as histograms. (b) Upregulation of ICAM-1 expression on SBC-3/ETP cells compared to SBC-3/ETP cells was also confirmed by IHC. Scale bar, 50 μm. (c) SCLC cells in biopsy specimens from chemonaïve patients heterogeneously expressing ICAM-1. Scale bar, 50 μm. (d) SBC-3/ETP cells were coincubated with YTS cells in the presence of 10 μg/ml of normal human IgG or trastuzumab (Tzmab) with or without 5 μg/ml of an anti-human ICAM-1 (CD54) Ab. Column, mean relative lysis ratio compared to that of normal IgG; bars, SD of three independent experiments; *, $P = 0.038$; **, $P = 0.026$; ***, $P = 0.025$. (e) Facilitation of trastuzumab-mediated ADCC by ICAM-1 is schematized. NK, natural killer cell; Mono, macrophage and monocyte; FcγR, Fcγ receptor.

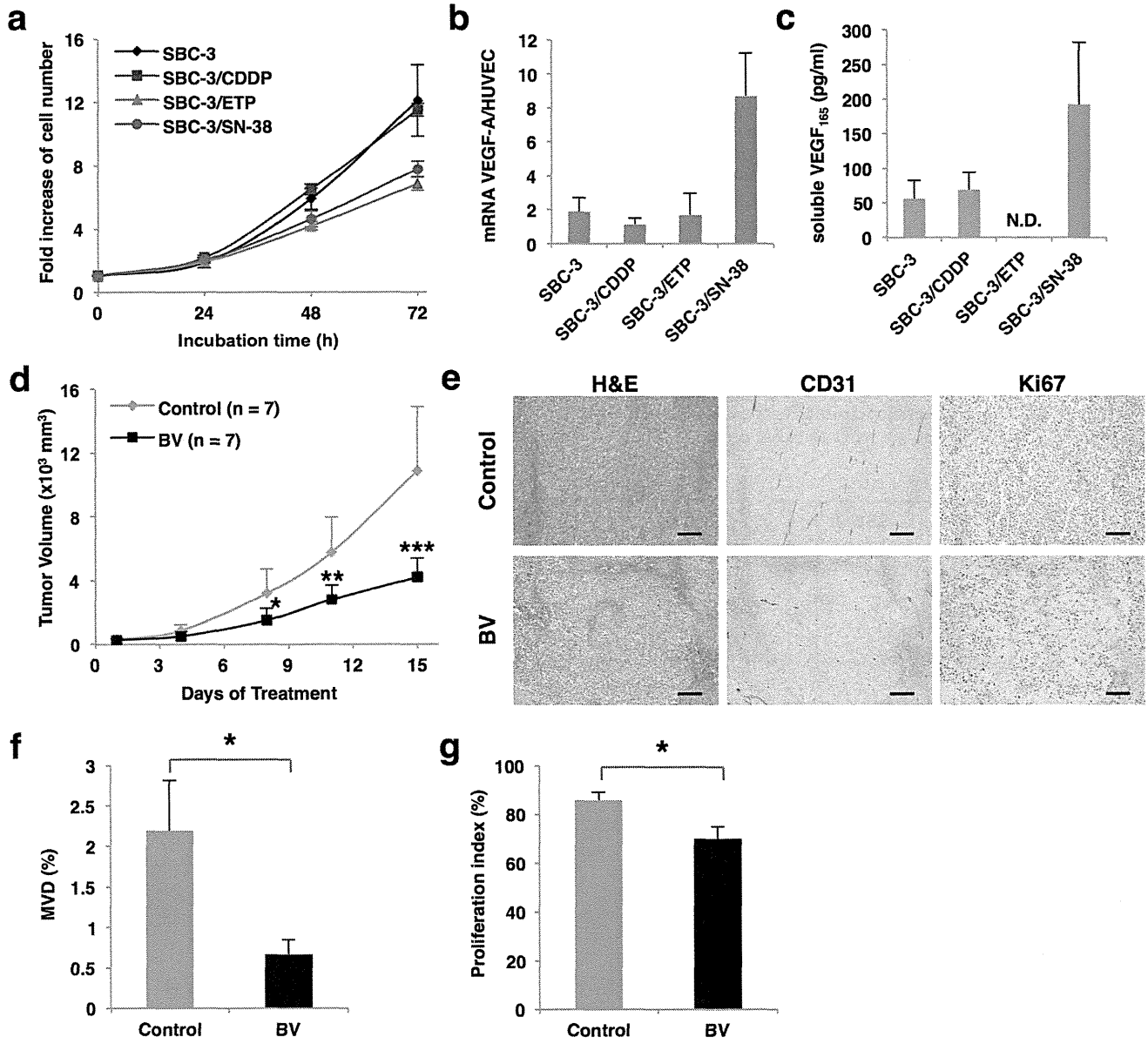

Figure 6 | Antitumor effects of bevacizumab against SBC-3/SN-38 xenografts. (a) *In vitro* proliferation assay of parental SBC-3 and SBC-3–derived chemoresistant cells. Points, mean fold increase in cell number; bars, SD from three experiments performed in triplicate. (b) VEGF-A mRNA expression in parental SBC-3 and SBC-3–derived chemoresistant cells was quantified by real-time PCR. Column, mean relative expression ratio to that of HUV-EC-C; bars, SD. (c) Soluble human $VEGF_{165}$ in the supernatants of each SCLC cell line was measured by ELISA. Column, mean concentration; bars, SD. Both experiments were performed at least thrice with triplicate samples. (d) SBC-3/SN-38 cells were inoculated into the flanks of athymic nude mice. When the tumor volume reached approximately 200–300 mm^3, the mice were randomly assigned to the PBS-treated control arm or bevacizumab (BV)-treated arm (n = 7 mice per group). Bevacizumab was intraperitoneally administered at a dose of 10 mg/kg twice weekly. Points, mean tumor volumes; bars, SD; *, $P = 0.031$; **, $P = 0.010$; ***, $P = 0.002$. (e) Representative H&E and IHC images for CD31 and Ki67. Scale bar, 100 μm. (f) MVD was determined based on the ratio of the CD31-positive area to the total observation area in five randomly selected fields. Column, mean; bars, SD; *, $P = 0.002$. (g) The proliferation index was determined by dividing the number of Ki67-positive cells by the total number of SCLC cells in five randomly selected fields. Column, mean; bars, SD; *, $P < 0.001$.

Methods

Clinical SCLC tissue samples. SCLC tissue samples were obtained by transbronchial or surgical biopsy from patients at Osaka University Hospital after institutional review board approval. All the patients provided written informed consent.

Antibodies and reagents. Trastuzumab and bevacizumab were provided by Chugai Pharmaceutical Co. (Tokyo, Japan). Rabbit polyclonal antibodies (Abs) against ubiquitin and actin (Santa Cruz Biotechnology, Santa Cruz, CA), Akt, phospho-Erk, and Erk (Cell Signaling Technology, Danvers, MA), and CD31 and Ki67 (Abcam, Cambridge, England) were used. Mouse monoclonal Abs against CD16 (3G8) and CD54 (HCD54) (BioLegend, San Diego, CA) and CD11a (Ancell, North Bayport, MN), rabbit monoclonal Abs against HER2 (D8F12), phospho-HER2 (6B12) and phospho-Akt (D9E) (Cell Signaling Technology), and rat monoclonal Ab against CD18 (YFC118.3) (Chemicon International, Temecula, CA) are also commercially available. Normal human IgG (Bethyl, Montgomery, TX) and horseradish peroxidase–conjugated goat anti-rabbit or anti-mouse IgG (BioRad, Hercules, CA) were also used. Cell Counting Kit-8 (CCK-8) and Cytotoxicity Detection Kit were obtained from Dojindo (Osaka, Japan) and Roche Applied Science (Penzberg, Upper Bavaria, Germany), respectively.

Cell lines and cell culture. The biological properties and the origin of SCLC cell lines, including H69, H446, N231, SBC-1, SBC-2, SBC-3, SBC-5, OS-1, OS2RA, OS3R5,

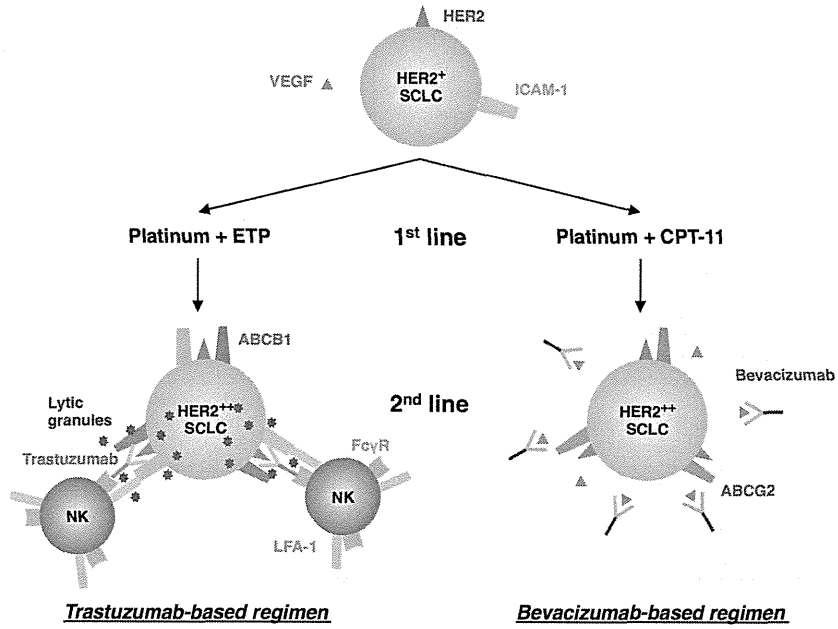

Figure 7 | Novel therapeutic decision tree to overcome chemoresistant SCLC based on HER2 expression. After HER2 is detected by IHC at the time of diagnosis, patients are divided into two groups according to the 1st line chemotherapy. Trastuzumab- or bevacizumab-based 2nd line chemotherapy is ideal for patients who have acquired resistance to etoposide-based or irinotecan-based 1st line chemotherapy, respectively. Upregulation of both HER2 and ICAM-1 in etoposide-resistant SCLC cells facilitates trastuzumab-mediated ADCC. Abundant VEGF produced from irinotecan-resistant SCLC cells is the main target of bevacizumab.

Smk, OC-10, and CADO LC6 as well as a breast carcinoma cell line, SK-BR-3, were previously described[19,36]. Chemoresistant sublines H69/CDDP[37] and H69/VP[38] were obtained from the National Cancer Center (Tokyo, Japan), while SBC-3/CDDP[39], SBC-3/ETP[40], and SBC-3/SN-38[41] were provided by Dr. K. Kiura (Okayama University, Okayama, Japan). A malignant non-Hodgkin's lymphoma cell line, NK92MI, was purchased from American Type Culture Collection (Rockville, MD). The characteristics of the natural killer leukemia cell lines YTS, a subline of YT, and NKL have been previously described[42–44]. HUV-EC-C cells were obtained from the Japan Health Sciences Foundation (Osaka, Japan). All SCLC cells, NKL cells, and YTS cells were maintained in RPMI 1640, and SK-BR-3 cells were maintained in McCOY's 5a supplemented with 10% heat-inactivated fetal bovine serum (FBS), penicillin (100 units/ml), and streptomycin (100 μg/ml). Interleukin-2 (100 units/ml), 1% sodium pyruvate, and 1% non-essential amino acids were also added to the NKL culture medium. HUV-EC-C cells were cultured in EBM-2 medium (Cambrex, Charles City, IA) supplemented with an EGM-2 kit containing 2% FBS, 0.04% hydrocortisone, 0.4% human basic fibroblast growth factor, 0.1% VEGF, and 0.1% heparin.

Immunohistochemistry (IHC). Four-μm thick sections were deparaffinized and incubated in Target Retrieval Solution pH 9.0 (Dako, Glostrup, Denmark) for 40 min at 96°C for antigen retrieval, after which endogenous peroxidase activity was blocked with Dako REAL peroxidase blocking (Dako). The sections were allowed to react with diluted primary Abs (1 : 50–100) overnight. Then, the slides were incubated with a peroxidase-labeled polymer conjugated to secondary anti-rabbit Abs using EnVision™+/HRP (Dako) and developed with 3,3′-deaminobenzidine as the chromogen. HercepTest (Dako) was performed according to the manufacturer's instructions.

Flow cytometry. To directly detect HER2 using trastuzumab, cells (2×10^5) were incubated with 1 μg of trastuzumab or control human IgG for 45 min at 4°C and then labeled with FITC-conjugated goat anti-human IgG (Abcam). To detect other cell surface proteins (CD54, CD16, CD11a, and CD18), cells (2×10^5) were stained with each properly diluted Ab (1 : 50–100) for 45 min at 4°C and then labeled with a FITC- or PE-conjugated secondary Ab. Stained cells were analyzed by FACSort (Becton Dickinson, Franklin Lakes, NJ). For CD16 detection, NK cells were preincubated with or without 10 μg/ml of trastuzumab for 4 h.

Trastuzumab sensitivity and cell proliferation assay. To evaluate the trastuzumab sensitivity of HER2-positive SCLC and SK-BR-3 cells, the cells (5×10^3 cells/well) were plated into 96-well tissue culture-treated plates (Corning) and treated with serially diluted trastuzumab or human IgG in serum-containing medium for 72 h. In the cell proliferation assay, the relative number of viable cells was quantified every 24 h using CCK-8 according to the manufacturer's instructions.

ADCC assay. In the ADCC assay, NK cell lines, including YTS, NKL[42–44], and NK92MI cells, were used as effector cells (E). In particular, CD16-positive YTS cells were sorted using FACSAria (Becton Dickinson) prior to the assay. SCLC cells (5×10^3 cells/well) as the target cells (T) were coincubated with NK cells at various E/T ratios with 10 μg/ml of trastuzumab or normal IgG in triplicate in 96-well plates. In the ICAM-1–blocking assay, 10 μg/ml of an anti-CD54–blocking Ab was also added. After 4-h incubation at 37°C, lactate dehydrogenase activity in the cell-free supernatants was measured using a Cytotoxicity Detection Kit and cytotoxicity was calculated according to manufacturer's instructions.

Trastuzumab internalization analysis. Cell surface–binding trastuzumab was analyzed by FACS as previously described[45]. Briefly, SCLC cells were incubated with 10 μg/ml of trastuzumab for 45 min at 4°C, and then either warmed to 37°C to allow internalization or maintained at 4°C. After internalization was stopped by transferring the cells to ice-cold buffer, cells were stained with FITC-conjugated goat anti-human IgG (Abcam) and analyzed by FACSort. The internalization rate was calculated as the mean fluorescence intensity (MFI) of the trastuzumab occupancy relative to that at the beginning of the internalization period using the formula $[(\mathrm{MFI}_{\text{measured trastuzumab occupancy}} - \text{background})/(\mathrm{MFI}_{\text{0 minutes trastuzumab occupancy}} - \text{background})] \times 100\%$.

To visualize trastuzumab internalization, cells grown on polyethyleneimine-coated cover glass (ASAHI GLASS, Tokyo, Japan) in 24-well plates (Corning, Corning, NY) were incubated with 50 nmol/l of Lysotracker (Lonza, Walkersville, MD) for 60 min at 37°C and then stained with 10 μg/ml of Alexa 488-labeled trastuzumab using an Alexa Fluor 488 monoclonal Ab labeling kit (Molecular Probes, Eugene, OR). Digital video images were collected under BZ-9000 (KEYENCE, Osaka, Japan) for up to 120 min and then analyzed using BZ-H2A software.

Immunoprecipitation and immunoblotting. Cells were either left untreated or treated with 10 μg/ml of trastuzumab for up to 240 min, and then lysed in lysis buffer. For immunoprecipitation analyses, whole cell lysates were precleared with 20 μl of protein G sepharose bead slurry (GE Healthcare, Buckinghamshire, UK), and then incubated with an anti-ubiquitin Ab (diluted 1 : 40) overnight at 4°C with gentle agitation. The immunoprecipitates were washed thrice in lysis buffer, denatured, and separated on a 5–20% gradient gel (Wako, Osaka, Japan) by SDS-PAGE and then transferred to a polyvinylidene difluoride membrane. The proteins were immunoblotted with an anti-HER2 rabbit monoclonal Ab (diluted 1 : 500) overnight at 4°C followed by the appropriate horseradish peroxidase–conjugated secondary Abs (diluted 1 : 10,000) for 1 h at room temperature. Immunoreactive bands were visualized using a chemiluminescent technique with ECL Plus Western Blotting Detection Reagents (GE Healthcare).

Quantitative reverse-transcription polymerase chain reaction (qRT-PCR). Total RNA was extracted using an RNeasy Mini Kit (Qiagen, Valencia, CA), and cDNA was

synthesized from 1 μg total RNA using High Capacity cDNA Reverse Transcription Kits (Applied Biosystems, Carlsbad, CA). qRT-PCR was performed with an Applied Biosystems Prism 7900HT Sequence Detection System using TaqMan® Universal PCR master mix according to the manufacturer's specifications (Applied Biosystems). The assay ID for the TaqMan primer set for human *VEGF-A* was no. Hs99999090_m1 (Applied Biosystems). Human *GAPDH* was used as an endogenous control (Applied Biosystems, Part Number 4352934E). Amplifications were performed in duplicate in ABI7900HT 96-well microtiter plates (Applied Biosystems). The thermal cycling conditions for the ABI7900HT were as follows: AmpErase UNG Activation for 2 min at 50°C, AmpliTaq God DNA Polymerase Activation for 10 min at 95°C, followed by 40 cycles each of Melt Anneal/Extend for 15 sec at 95°C and 1 min at 60°C.

Enzyme-linked immunosorbent assay (ELISA). Cells (3×10^4 cells/well) were plated into 24-well tissue culture–treated plates (Corning) in triplicate and allowed to proliferate for 24 h. Then, the supernatants of each well were collected, and the levels of human $VEGF_{165}$ were measured using Quantikine kits (R&D Systems, Minneapolis, MN) according to the manufacturer's protocol.

Treatment of HER2-positive SCLC xenografts. All animal experiments were approved by The Institute of Experimental Animal Sciences Osaka University Medical School. Six-to-eight week old male BALB/cA Jcl nu/nu mice were obtained from CLEA Japan (Osaka, Japan). SCLC cells ($1–2 \times 10^7$) were inoculated subcutaneously into the flanks of mice. When the tumor volume reached approximately 200–300 mm^3, the mice were randomly assigned into one of two treatment groups and either treated with intraperitoneal injections of PBS or 30 mg/kg of trastuzumab twice weekly to evaluate the antitumor activity of trastuzumab[46], or PBS or 10 mg/kg of bevacizumab twice weekly to the evaluate antitumor activity of bevacizumab[47]. Tumor volume (V) was calculated using the following equation: V (mm^3) = length × (width)^2/2. Mice were sacrificed by CO_2 inhalation, and tumor samples were resected by the 50th treatment day for histological analyses.

TUNEL staining. TUNEL staining was performed to measure apoptosis in paraffin-embedded tumor sections using ApopTag Peroxidase In Situ Apoptosis Detection kit according to the manufacturer's instructions (Merck Millipore, Billerica, MA). Cell nuclei were stained with methyl green.

Micro vessel density (MVD) assessment. MVD (%) was calculated based on the ratio of the CD31-positive area to the total observation area in the viable region. At least five fields per section were randomly analyzed, excluding necrotic areas. Quantification was performed using imaging analysis software (NIS-Elements D3.00, Nicon Instruments Company, Tokyo, Japan).

Statistical analysis. All statistical evaluations were performed in triplicate for each experiment and repeated at least thrice. Mean ± SD values were calculated, and differences were evaluated using two-sided Student's *t* test. $P < 0.05$ was considered statistically significant.

1. Rodriguez, E. & Lilenbaum, R. C. Small cell lung cancer: past, present, and future. *Curr Oncol Rep* **12**, 327–334 (2010).
2. Hanna, N. H. & Einhorn, L. H. Small-cell lung cancer: state of the art. *Clin Lung Cancer* **4**, 87–94 (2002).
3. Noda, K. *et al.* Irinotecan plus cisplatin compared with etoposide plus cisplatin for extensive small-cell lung cancer. *N Engl J Med* **346**, 85–91 (2002).
4. Rossi, A., Martelli, O. & Di Maio, M. Treatment of patients with small-cell lung cancer: from meta-analyses to clinical practice. *Cancer Treat Rev* **39**, 498–506 (2013).
5. Johnson, B. E. *et al.* Phase II study of imatinib in patients with small cell lung cancer. *Clin Cancer Res* **9**, 5880–5887 (2003).
6. Moore, A. M. *et al.* Gefitinib in patients with chemo-sensitive and chemo-refractory relapsed small cell cancers: a Hoosier Oncology Group phase II trial. *Lung Cancer* **52**, 93–97 (2006).
7. Fischer, B., Marinov, M. & Arcaro, A. Targeting receptor tyrosine kinase signalling in small cell lung cancer (SCLC): what have we learned so far? *Cancer Treat Rev* **33**, 391–406 (2007).
8. Ménard, S., Tagliabue, E., Campiglio, M. & Pupa, S. M. Role of HER2 gene overexpression in breast carcinoma. *J Cell Physiol* **182**, 150–162 (2000).
9. Slamon, D. J. *et al.* Studies of the HER-2/neu proto-oncogene in human breast and ovarian cancer. *Science* **244**, 707–712 (1989).
10. Ross, J. S. & Fletcher, J. A. The HER-2/neu oncogene in breast cancer: prognostic factor, predictive factor, and target for therapy. *Stem Cells* **16**, 413–428 (1998).
11. Micke, P. *et al.* c-erbB-2 expression in small-cell lung cancer is associated with poor prognosis. *Int J Cancer* **92**, 474–479 (2001).
12. Potti, A. *et al.* Predictive role of HER-2/neu overexpression and clinical features at initial presentation in patients with extensive stage small cell lung carcinoma. *Lung Cancer* **36**, 257–261 (2002).
13. Slamon, D. J. *et al.* Use of chemotherapy plus a monoclonal antibody against HER2 for metastatic breast cancer that overexpresses HER2. *N Engl J Med* **344**, 783–792 (2001).
14. Bang, Y. J. *et al.* Trastuzumab in combination with chemotherapy versus chemotherapy alone for treatment of HER2-positive advanced gastric or gastro-oesophageal junction cancer (ToGA): a phase 3, open-label, randomised controlled trial. *Lancet* **376**, 687–697 (2010).
15. Jones, K. L. & Buzdar, A. U. Evolving novel anti-HER2 strategies. *Lancet Oncol* **10**, 1179–1187 (2009).
16. Clynes, R. A., Towers, T. L., Presta, L. G. & Ravetch, J. V. Inhibitory Fc receptors modulate in vivo cytotoxicity against tumor targets. *Nat Med* **6**, 443–446 (2000).
17. Lagadec, P. F., Saraya, K. A. & Balkwill, F. R. Human small-cell lung-cancer cells are cytokine-resistant but NK/LAK-sensitive. *Int J Cancer* **48**, 311–317 (1991).
18. Savas, B., Kerr, P. E., Ustun, H., Cole, S. P. & Pross, H. F. Lymphokine-activated killer cell susceptibility and multidrug resistance in small cell lung carcinoma. *Anticancer Res* **18**, 4355–4361 (1998).
19. Minami, T. *et al.* HER2 as Therapeutic Target for Overcoming ATP-binding Cassette Transporter-Mediated Chemoresistance in Small Cell Lung Cancer. *Mol Cancer Ther* **11**, 830–841 (2012).
20. Wolff, A. C. *et al.* American Society of Clinical Oncology/College of American Pathologists guideline recommendations for human epidermal growth factor receptor 2 testing in breast cancer. *J Clin Oncol* **25**, 118–145 (2007).
21. Ross, J. S. *et al.* The HER-2 receptor and breast cancer: ten years of targeted anti-HER-2 therapy and personalized medicine. *Oncologist* **14**, 320–368 (2009).
22. Ganti, A. K. & Panwalkar, A. W. Targeted therapy for small cell lung cancer. *Targ Oncol* **2**, 89–97 (2007).
23. Rüschoff, J. *et al.* HER2 testing in gastric cancer: a practical approach. *Mod Pathol* **25**, 637–650 (2012).
24. Vogel, C. L. *et al.* Efficacy and safety of trastuzumab as a single agent in first-line treatment of HER2-overexpressing metastatic breast cancer. *J Clin Oncol* **20**, 719–726 (2002).
25. Baselga, J. *et al.* Phase II study of efficacy, safety, and pharmacokinetics of trastuzumab monotherapy administered on a 3-weekly schedule. *J Clin Oncol* **23**, 2162–2171 (2005).
26. Paik, S., Kim, C. & Wolmark, N. HER2 status and benefit from adjuvant trastuzumab in breast cancer. *N Engl J Med* **358**, 1409–1411 (2008).
27. Helander, T. S. & Timonen, T. Adhesion in NK cell function. *Curr Top Microbiol Immunol* **230**, 89–99 (1998).
28. Barber, D. F., Faure, M. & Long, E. O. LFA-1 contributes an early signal for NK cell cytotoxicity. *J Immunol* **173**, 3653–3659 (2004).
29. Bryceson, Y. T., March, M. E., Barber, D. F., Ljunggren, H. G. & Long, E. O. Cytolytic granule polarization and degranulation controlled by different receptors in resting NK cells. *J Exp Med* **202**, 1001–1012 (2005).
30. Bryceson, Y. T., March, M. E., Ljunggren, H. G. & Long, E. O. Activation, coactivation, and costimulation of resting human natural killer cells. *Immunol Rev* **214**, 73–91 (2006).
31. Ready, N. E. *et al.* Cisplatin, irinotecan, and bevacizumab for untreated extensive-stage small-cell lung cancer: CALGB 30306, a phase II study. *J Clin Oncol* **29**, 4436–4441 (2011).
32. Spigel, D. R. *et al.* Randomized phase II study of bevacizumab in combination with chemotherapy in previously untreated extensive-stage small-cell lung cancer: results from the SALUTE trial. *J Clin Oncol* **29**, 2215–2222 (2011).
33. Burris, H. A., 3rd. *et al.* Phase II study of the antibody drug conjugate trastuzumab-DM1 for the treatment of human epidermal growth factor receptor 2 (HER2)-positive breast cancer after prior HER2-directed therapy. *J Clin Oncol* **29**, 398–405 (2011).
34. Teicher, B. A. & Chari, R. V. Antibody conjugate therapeutics: challenges and potential. *Clin Cancer Res* **17**, 6389–6397 (2011).
35. Junttila, T. T., Li, G., Parsons, K., Phillips, G. L. & Sliwkowski, M. X. Trastuzumab-DM1 (T-DM1) retains all the mechanisms of action of trastuzumab and efficiently inhibits growth of lapatinib insensitive breast cancer. *Breast Cancer Res Treat* **128**, 347–356 (2011).
36. Mitsuhashi, Y., Inaba, M., Sugiyama, Y. & Kobayashi, T. In vitro measurement of chemosensitivity of human small cell lung and gastric cancer cell lines toward cell cycle phase-nonspecific agents under the clinically equivalent area under the curve. *Cancer* **70**, 2540–2546 (1992).
37. Hong, W. S. *et al.* Establishment and characterization of cisplatin-resistant sublines of human lung cancer cell lines. *Int J Cancer* **41**, 462–467 (1988).
38. Minato, K. *et al.* Characterization of an etoposide-resistant human small-cell lung cancer cell line. *Cancer Chemother Pharmacol* **26**, 313–317 (1990).
39. Moritaka, T. *et al.* Cisplatin-resistant human small cell lung cancer cell line shows collateral sensitivity to vinca alkaloids. *Anticancer Res* **18**, 927–933 (1998).
40. Takigawa, N., Ohnoshi, T., Ueoka, H., Kiura, K. & Kimura, I. Establishment and characterization of an etoposide-resistant human small cell lung cancer cell line. *Acta Med Okayama* **46**, 203–212 (1992).
41. Chikamori, M. *et al.* Establishment of a 7-ethyl-10-hydroxy-camptothecin-resistant small cell lung cancer cell line. *Anticancer Res* **24**, 3911–3916 (2004).
42. Drexler, H. G. & Matsuo, Y. Malignant hematopoietic cell lines: in vitro models for the study of natural killer cell leukemia-lymphoma. *Leukemia* **14**, 777–782 (2000).
43. Chen, X. *et al.* CD28-stimulated ERK2 phosphorylation is required for polarization of the microtubule organizing center and granules in YTS NK cells. *Proc Natl Acad Sci U S A* **103**, 10346–10351 (2006).
44. Robertson, M. J. *et al.* Characterization of a cell line, NKL, derived from an aggressive human natural killer cell leukemia. *Exp Hematol* **24**, 406–415 (1996).
45. Lammerts van Bueren, J. J. *et al.* Effect of target dynamics on pharmacokinetics of a novel therapeutic antibody against the epidermal growth factor receptor: implications for the mechanisms of action. *Cancer Res* **66**, 7630–7638 (2006).

46. Baselga, J., Norton, L., Albanell, J., Kim, Y. M. & Mendelsohn, J. Recombinant humanized anti-HER2 antibody (Herceptin) enhances the antitumor activity of paclitaxel and doxorubicin against HER2/neu overexpressing human breast cancer xenografts. *Cancer Res* **58**, 2825–2831 (1998).
47. Cascone, T. *et al.* Upregulated stromal EGFR and vascular remodeling in mouse xenograft models of angiogenesis inhibitor-resistant human lung adenocarcinoma. *J Clin Invest* **121**, 1313–1328 (2011).

Acknowledgements

We thank Dr. K. Kiura (Okayama University, Okayama, Japan) for kindly providing SBC-3 and its chemoresistant sublines. This work was supported by Grant-in-Aid for Scientific Research (C) from the Ministry of Education, Culture, Sports, Science and Technology, Japan (24591165; T. K.) and also by Funding Program for Next Generation World-Leading Researchers (NEXT Program), Core Research for Evolutional Science and Technology, Japan Science and Technology Agency (CREST JST), and Special Coordination Funds for Promoting Science and Technology, Japan.

Author contributions

T.M. and T.K. conceived the study and designed experiments; T.M., S.K., Y.O., I.N. and S.I. carried out experiments; T.M., T.K., R.T., K.M., M.H., O.M., K.T. and H.H. collected tumor samples from patients; H.A. and A.K. interpreted and advised on immunological experiments; T.M., T.K., S.K., K.I., Y.T., H.K., I.T. analyzed the data; T.M., T.K. and A.K. wrote the manuscript, which was reviewed and edited by the other coauthors.

Additional information

Supplementary information accompanies this paper at http://www.nature.com/scientificreports

Competing financial interests: The authors declare no competing financial interests.

How to cite this article: Minami, T. *et al.* Overcoming chemoresistance of small-cell lung cancer through stepwise HER2-targeted antibody-dependent cell-mediated cytotoxicity and VEGF-targeted antiangiogenesis. *Sci. Rep.* **3**, 2669; DOI:10.1038/srep02669 (2013).

Lung Cancer 82 (2013) 299–304

Contents lists available at ScienceDirect

Lung Cancer

journal homepage: www.elsevier.com/locate/lungcan

A retrospective analysis of 335 Japanese lung cancer patients who responded to initial gefitinib treatment

K. Nishino[a,*], F. Imamura[a], S. Morita[b], M. Mori[c], K. Komuta[d], T. Kijima[e], Y. Namba[c], T. Kumagai[a], S. Yamamoto[d], I. Tachibana[e], Y. Nakazawa[c], J. Uchida[a], S. Minami[d], R. Takahashi[e], Y. Yano[c], T. Okuyama[a], A. Kumanogoh[e]

[a] Department of Thoracic Oncology, Osaka Medical Center for Cancer and Cardiovascular Diseases, Osaka, Japan
[b] Department of Biostatistics and Epidemiology, Yokohama City University Graduate School of Medicine, Kanagawa, Japan
[c] Department of Respiratory Medicine, National Hospital Organization Toneyama National Hospital, Osaka, Japan
[d] Department of Respiratory Medicine, Osaka Police Hospital, Osaka, Japan
[e] Department of Respiratory Medicine, Allergy and Rheumatic Diseases, Osaka University Graduate School of Medicine, Osaka, Japan

ARTICLE INFO

Article history:
Received 23 May 2013
Received in revised form 5 August 2013
Accepted 7 August 2013

Keywords:
Responders to gefitinib
Long survival
Rechallenge
Beyond progressive disease
Nonsmall-cell lung cancer
EGFR-tyrosine kinase inhibitor

ABSTRACT

Background: Gefitinib treatment results in considerably better progression-free survival compared with that of platinum doublets in the first line treatment of nonsmall-cell lung cancer (NSCLC) carrying an activating epidermal growth factor receptor (*EGFR*) mutation. Some patients who respond to gefitinib have an overall survival (OS) of more than 5 years, whereas other initial responders do less well. Although there has been considerable effort made to elucidate the mechanisms of acquired resistance, there have only been a few studies that addressed the effect of clinical backgrounds and treatment histories on the survival of the patients who had responded to an EGFR-tyrosine kinase inhibitor (TKI). In this study, we especially focused on the clinical benefit of EGFR-TKI administration after progression.
Patients and methods: We retrospectively analyzed consecutive patients with advanced NSCLC who were diagnosed before October 2010, treated with gefitinib after July 2002, and responded to it. The primary objective of this study was to evaluate how clinical backgrounds and treatment histories influence survival of the patients who respond to gefitinib. The secondary objectives were to evaluate the safety of long-term gefitinib use and to establish the optimal treatment sequence using a dynamic treatment regimen analysis (DTRA).
Results: A total of 335 patients were recruited. Twenty-eight (8.4%) patients survived more than 5 years. Sixty-five and 93 patients received gefitinib as rechallenge and beyond progressive disease (BPD), respectively. A statistically significant difference in OS was observed between the patients who underwent gefitinib rechallenge and those who did not rechallenge (median: 1272 days *vs.* 774 days; $p < 0.001$), a result supported by a DTRA. Patients treated with gefitinib BPD also showed a tendency of longer survival.
Conclusions: Gefitinib rechallenge and BPD played a central role in long term survival of the patients who initially responded to gefitinib.

1. Introduction

Platinum-based chemotherapy is the standard first line treatment for patients with advanced nonsmall-cell lung cancer (NSCLC), but its efficacy is considered to be low with the median overall survival (OS) of only 8–12 months [1,2]. The discovery of activating mutations of the *epidermal growth factor receptor* (*EGFR*) gene and the clinical application of EGFR-tyrosine kinase inhibitors (TKIs) such as gefitinib and erlotinib have opened a new paradigm for the treatment of advanced NSCLC [3,4]. Two recent randomized studies (NEJ002 and WJTOG3405) have shown that the progression-free survival (PFS) of the patients treated with gefitinib is longer than that of those treated with platinum-doublets in the first line treatment for advanced NSCLC harboring activating *EGFR* mutations [5,6]. Response rates exceeded 70% with gefitinib, and a median PFS was approximately 10 months [7]. Similarly, superiority of erlotinib over platinum doublets as a first line treatment has been demonstrated by 2 phase III studies (OPTIMAL and EURTAC) [8,9]. The median OS exceeds 2 years in these studies.

Despite these advances, OS of the patients who respond to first line gefitinib therapy differ widely. Although a variety of clinical factors and backgrounds probably influence on patient survival, it is

* Corresponding author at: Department of Thoracic Oncology, Osaka Medical Center for Cancer and Cardiovascular Diseases, 1-3-3 Nakamichi Higashinari-ku, Osaka 537-8511, Japan. Tel.: +81 6 6972 1181; fax: +81 6 6971 7636.
E-mail address: nishinishipptruth@yahoo.co.jp (K. Nishino).

0169-5002/$ – see front matter © 2013 Elsevier Ireland Ltd. All rights reserved.
http://dx.doi.org/10.1016/j.lungcan.2013.08.009

still unknown which of these are critical. Recently, there have been several reports on the relevance of novel strategies such as rechallenge of an EGFR-TKI [10] and the continuation of an EGFR-TKI beyond the Response Evaluation Criteria in Solid Tumors (RECIST) progressive disease (BPD) [11,12]. Although these strategies may have a clinical impact on OS, the number of the patients in each of these studies was too small to conclude which strategy is the most beneficial.

In this study, we retrospectively analyzed 335 Japanese responders to initial gefitinib therapy in order to identify the factor which contributed to a prolongation of OS. We were particularly focused on the contribution of EGFR-TKIs as rechallenge and BPD.

2. Patients and methods

2.1. Patients

Patients who were diagnosed with advanced NSCLC before October 2010 and treated with gefitinib after July 2002 were recruited consecutively. The inclusion criteria were that the patient should have cytologically or histologically proved advanced NSCLC diagnosed by October 2010, have received gefitinib treatment starting after July 2002 (the date when gefitinib was approved in Japan), and have an initial clinical stage of III or IV and an Eastern Cooperative Oncology Group (ECOG) performance status (PS) grade 0–2 at the initial presentation. In addition, patients should have experienced a clinical benefit from initial gefitinib therapy (the responders), defined as a complete response (CR), a partial response (PR), or stable disease (SD) lasting at least for 6 months. Patients were excluded if they had undergone radical surgery or curative radiation therapy.

2.2. Study design

This is a retrospective but protocol-based study. The primary objective was to evaluate how clinical backgrounds and treatment histories relate to survival benefit for the responders to gefitinib. The secondary objective was to evaluate the best way to administer gefitinib, gefitinib rechallenge and BPD. We defined rechallenge of gefitinib as its re-administration after treatment with 1 or more cytotoxic chemotherapy regimens following initial gefitinib failure. Gefitinib BPD was defined as the continuation of gefitinib for at least 1 month after gefitinib failure determined by RECIST version 1.0. This study was performed in accordance with the Declaration of Helsinki, "Ethics Guidelines for Clinical Research (Public Notice of the Ministry of Health, Labor, and Welfare, No. 415 of 2008)," and "Ethics Guidelines for Epidemiology (Public Notice of the Ministry of Health, Labor, and Welfare, No. 291 of 2004)". This study was registered as UMIN000006913.

2.3. Data collection

Patient backgrounds were extracted from the medical records. These included gender, age, histology, clinical stage at diagnosis, metastatic sites, the date of diagnosis, Eastern Cooperative Oncology Group performance status (ECOG PS) at the initial presentation, smoking status, and *EGFR* mutation status. The information of chemotherapy regimens for NSCLC, the site and the dose of irradiation, and the dates of the first and the last administration of each treatment were also collected. Toxicities of grade 3 or higher (≥grade 3 toxicities) of gefitinib were evaluated according to the National Cancer Institute's Common Terminology Criteria for Adverse Events (CTCAE) version 4.0. The best response and PFS time were determined for each treatment with reference to RECIST version 1.0. The data cut-off date was October 31, 2011, when the survival status of the patients was determined.

2.4. Statistical analysis

Statistical analysis was performed using SAS for Windows version 9.2 (SAS Institute Inc., Cary, NC, USA). OS and PFS were analyzed using the Kaplan–Meier method and log-rank test. Multivariate analysis of survival data was performed by a Cox hazards model using the following covariates: gender, age, stage, histology, ECOG PS grade, smoking status, *EGFR* mutation status, and the presence or absence of rechallenge and BPD.

In daily practice, a chemotherapy regimen is usually selected based on multiple factors including the current PS, residual toxicities of preceding chemotherapy, and the response to prior therapies. A conventional Cox proportional hazards model is insufficient to explore the key treatment strategy that contributes to long-term survival in an unbalanced retrospective cohort study. To solve this issue, we performed a dynamic treatment regimen analysis (DTRA) as it allows a comparison that takes not only baseline characteristics but also time-dependent covariates into consideration [13,14]. In addition, a DTRA makes it possible to compare the effects of multiple treatment strategies or sequences on time-to-event data like OS in a non-randomized observational study context [15]. In this study, a DRTA was applied to compare the sequence of 3 consecutive chemotherapy regimens starting from the initial administration of gefitinib to see which sequence was associated with the longest OS. Covariates used in the DTRA were gender, age, PS, smoking status, histology, stage, and the responses to the first and second treatments in the target sequence.

3. Results

3.1. Patient characteristics

A total of 335 patients were enrolled in the study. Twenty-eight (8.4%), 40 (11.9%) and 76 (22.7%) patients survived more than 5, 4 and 3 years, respectively. The longest survival time was 3867 days, achieved by a patient who had received 10 regimens including gefitinib administration with 496-days duration. The patient characteristics are summarized in Table 1. The median age was 68 years. Patients included 237 (70.7%) women, 217 (64.8%) never-smokers, 231 (69.0%) with ECOG PS 1, and 299 (89.2%) with adenocarcinoma. *EGFR* mutation status was evaluated in 137 (40.9%) patients. There were no significant differences in patient characteristic except the *EGFR* mutation status between all patients and the survivors of more than 3-, 4-, and 5-years (Table 1). Less activated *EGFR* mutation was observed in the patients who survived more than 3-, 4-, and 5-years compared with that in overall patients.

3.2. Treatment sequences and exposure to gefitinib

Fig. 1 shows the treatment sequences in all patients. The gefitinib treatment occupies 46.9% of the total treatment period. The occupancy by treatment with EGFR-TKIs increases to 65.3% when erlotinib was also taken into account. The median duration of gefitinib treatment was 267 days in all patients (range, 4–3131 days), whereas it was 926 days (range, 169–3131 days) in the 5-year survivors (Table 2). Fourteen (50%) and 11 (39.3%) of the 5-year survivors were treated with gefitinib rechallenge and gefitinib BPD, respectively. In long-term survivors, significantly more patients underwent gefitinib rechallenge. The percentage of the patients who experienced gefitinib BPD appears to be higher in long-term survivors, although this is not statistically significant.

Table 1
Clinical characteristics.

Characteristics	All patients	Long-term survivors					
	n (%)	≥3 years		≥4 years		≥5 years	
	335 (100)	76 (100)	*p*	40 (100)	*p*	28 (100)	*p*
Gender							
Male	98 (29.3)	15 (19.7)	0.093	7 (17.5)	0.118	3 (10.7)	0.035
Female	237 (70.7)	61 (80.3)		33 (82.5)		25 (89.3)	
Age							
Mean	68	61.3	0.03	61.5	0.139	61.5	0.097
Range	20–84	20–78		43–78		43–74	
Smoking status							
Never	217 (64.8)	56 (73.7)	0.325	31 (77.5)	0.268	22 (78.6)	0.287
Current	108 (32.2)	18 (23.7)		8 (20.0)		5 (17.9)	
Unknown	10 (3.0)	2 (2.6)		1 (2.5)		1 (3.6)	
Stage							
IIIA	5 (1.5)	1 (1.3)	0.405	0	0.377	0	0.429
IIIB	65 (19.4)	20 (26.3)		11 (27.5)		8 (28.6)	
IV	265 (79.1)	55 (72.4)		29 (72.5)		20 (71.4)	
ECOG PS							
0	61 (18.2)	20 (26.3)	0.236	11 (27.5)	0.464	9 (32.1)	0.210
1	231 (69.0)	51 (67.1)		26 (65.0)		18 (64.3)	
2	42 (12.5)	5 (6.6)		3 (7.5)		1 (3.6)	
Unknown	1 (0.3)	0		0		0	
Histology							
Adeno	299 (89.2)	69 (90.8)	0.486	37 (92.5)	0.118	26 (93.9)	0.235
Squamous	24 (7.2)	3 (3.9)		0		0	
Others	12 (3.6)	4 (5.3)		3 (7.5)		2 (7.1)	
EGFR mutation status							
Activating mutation	127 (37.9)	14 (18.4)	0.005	6 (15.0)	0.009	4 (14.3)	0.043
Wild type	10 (3.0)	4 (5.3)		3 (7.5)		1 (3.6)	
Unknown	198 (59.1)	58 (76.3)		31 (77.5)		23 (82.1)	

Abbreviations. ECOG PS, Eastern Cooperative Oncology Group performance status; *EGFR*, epidermal growth factor receptor; adeno, adenocarcinoma; squamous, squamous cell carcinoma; *p*, *p*-value, comparison with overall population.

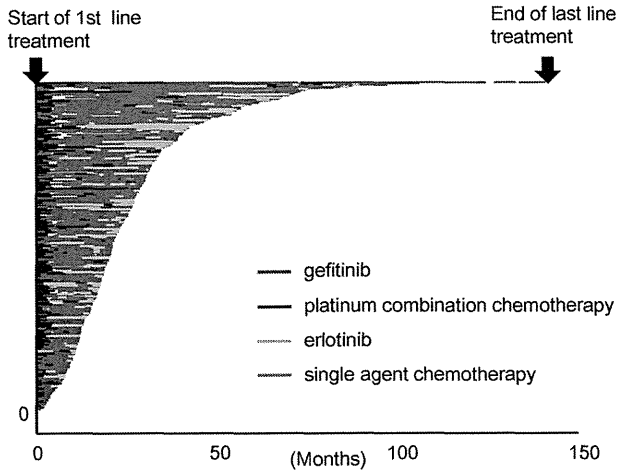

Fig. 1. Treatment sequence for all patients.

3.3. Gefitinib-related adverse events

All 335 patients were assessed for ≥grade 3 toxicities of gefitinib. The most common ≥grade 3 adverse event was hepatic toxicity, observed in 41 patients (12.2%). Interstitial lung disease (ILD) occurred in 10 patients (3%), of whom 5 died as a result. In 8 of 10 (80%) patients with ILD, it developed within 3 months after starting the first gefitinib treatment, which is similar to the findings of previous studies [5,6]. ILD occurred in 1 (1.5%) of the patients during gefitinib rechallenge. It is notable that most adverse events developed within 3 months, and their profile and severity were similar even after long-term administration.

3.4. Impact of gefitinib rechallenge and BPD on OS

The median OS of 65 patients who experienced gefitinib rechallenge was 1272 days compared with 774 days for those who did not. The mortality rechallenge was significantly reduced in the patients who received gefitinib rechallenge with hazard ratio (HR) of 0.519

Table 2
Exposure to gefitinib.

Number	All patients	Long-term survivors		
	335	≥3 years 76 (22.7%)	≥4 years 40 (11.9%)	≥5 years 28 (8.4%)
Duration of gefitinib treatment (days)				
Median	267	578	848	926
Range	4–3131	33–3131	33–3131	169–3131
Gefitinib rechallenge	65 (19.4%)	32 (42.1%)	18 (45.0%)	14 (50.0%)
p-Value		<0.001	<0.001	<0.001
Gefitinib BPD	93 (27.8%)	26 (34.2%)	13 (32.5%)	11 (39.3%)
p-Value		0.263	0.529	0.195

Abbreviation. BPD, beyond RECIST progressive disease.
p-Value: comparison with overall population.

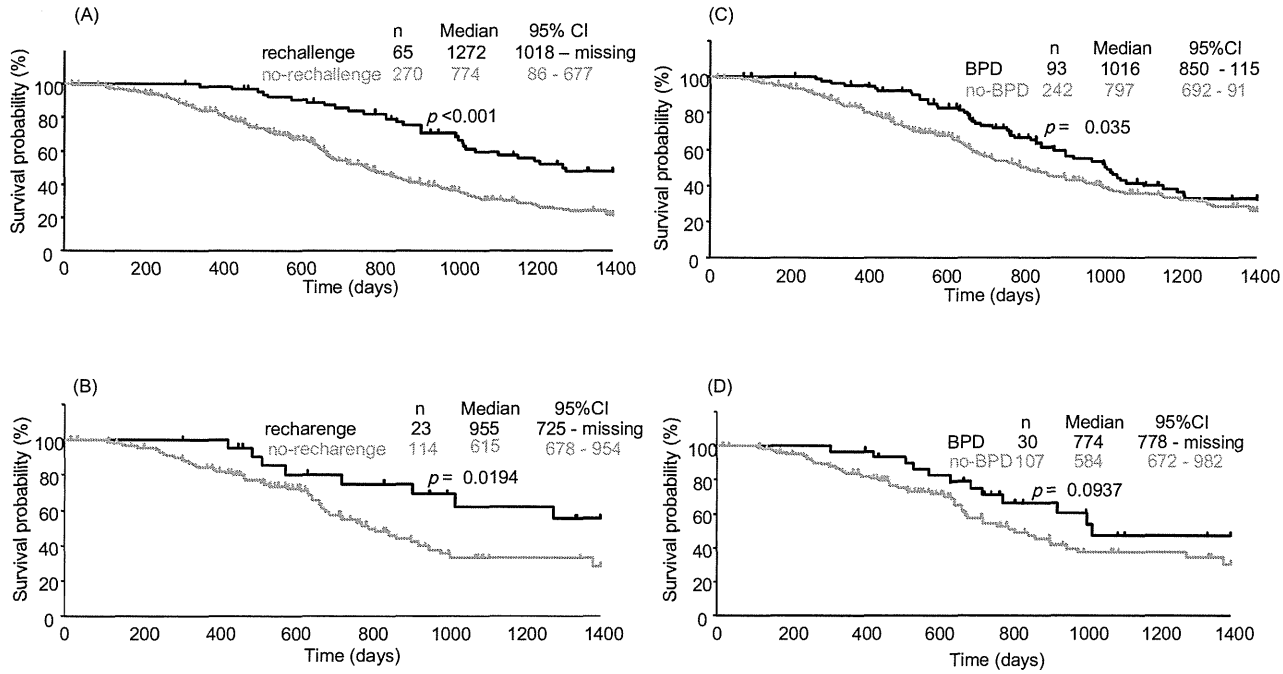

Fig. 2. Kaplan–Meier curves. (A) Overall survival (OS) of all patients ($n = 335$) with and without gefitinib rechallenge, (B) OS of the patients with known *EGFR* mutation status ($n = 137$) with and without gefitinib rechallenge, (C) OS of all patients ($n = 335$) with and without gefitinib beyond progressive disease (BPD) and (D) OS of the patients with known *EGFR* mutation status ($n = 137$) with and without gefitinib BPD.

($p < 0.001$) (Fig. 2A). Multivariate analysis showed that rechallenge was associated with a significant improvement of OS (HR = 0.528, 95% confidence interval (CI): 0.373–0.747; $p = 0.0003$) (Table 3). The DTRA revealed that the sequence of gefitinib, chemotherapy, and gefitinib rechallenge prolonged OS by 46 days on average compared with that of gefitinib, chemotherapy, and chemotherapy, although this increase was not statistically significant (Fig. 3). Ninety-three patients were treated with gefitinib BPD either with (18.3%) or without (81.7%) the co-administration of cytotoxic drugs. The OS of the cohort with BPD was longer than that without BPD (HR = 0.726, 95% CI: 0.538–0.980; $p = 0.035$), with a median OS of 1016 days and 797 days, respectively (Fig. 2C). Multivariate analysis showed that BPD was not associated with a significant improvement of OS (HR = 0.808, 95% CI: 0.589–1.110; $p = 0.1886$).

The *EGFR* mutation status was known in 137 patients. Twenty-three of them received gefitinib rechallenge, and their OS of 955 days was long compared with 615 days for those without rechallenge (Fig. 2B). The mortality was significantly reduced with HR = 0.422 ($p = 0.0194$). Multivariate analysis revealed gefitinib rechallenge, together with stage and PS, was a significant and independent prognostic factor in the patients with known *EGFR* mutation status (HR = 0.432, 95% CI: 0.198–0.944; $p = 0.0353$). Any other variables such as gender, age, and even *EGFR* mutation status were not associated with OS (Table 3). Thirty patients with known

Table 3
Cox analysis of overall survival (gefitinib rechallenge).

Variables	Multivariate analysis (overall survival)					
	All patients ($n = 335$)			Patients with known *EGFR* mutation status ($n = 137$)		
	HR	95% CI	p	HR	95% CI	p
Gender						
Female/male	0.877	0.627–1.228	0.4451	0.963	0.448–2.070	0.9237
Stage						
IV/IIIB	1.350	0.941–1.938	0.1034	3.164	1.444–6.933	0.0040
Age						
51–60/≤50	0.779	0.466–1.300	0.0241	1.074	0.377–3.058	0.7994
61–70/≤50	0.984	0.604–1.603		0.844	0.347–2.053	
71–80/≤50	1.316	0.791–2.190		1.242	0.496–3.107	
≥81/≤50	2.195	0.985–4.891		1.290	0.364–4.565	
PS						
Continuous value	1.149	0.984–1.341	0.0787	1.848	1.2405–2.834	0.0049
Smoking status						
Continuous value	1.109	1.012–1.215	0.0266	1.160	0.937–1.437	0.1727
EGFR mutation status						
M(+)/M(−)	1.250	0.586–2.664	0.7363	1.202	0.520–2.782	0.6671
Unknown/M(−)	1.321	0.635–2.746		–	–	–
Rechallenge						
Yes/no	0.528	0.373–0.747	0.0003	0.432	0.198–0.944	0.0353

Abbreviations. HR, hazard ratio; CI, confidence interval; p, p-value; M(+), *EGFR* mutation positive; M(−), *EGFR* mutation negative (wild type).

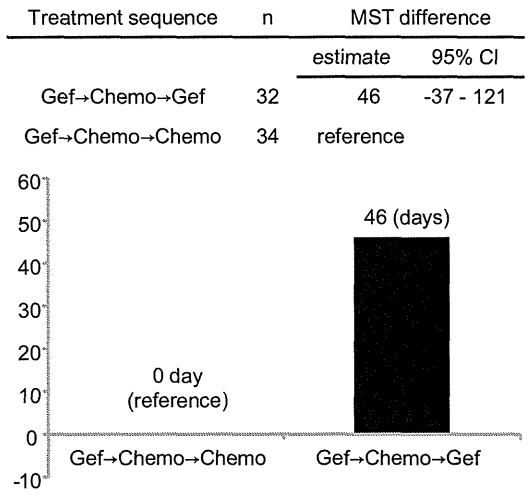

Fig. 3. Dynamic treatment regimen analysis (DTRA). *Abbreviations.* Gef, gefitinib; Chemo, chemotherapy; MST, median survival time.

EGFR mutation status were treated with gefitinib BPD. As shown in Fig. 2D, there was no significant difference of OS between two groups with and without gefitinib BPD ($p = 0.0937$).

4. Discussion

To the best of our knowledge, our study is the largest retrospective analysis comparing gefitinib rechallenge and BPD for patients who initially responded to it. The long-term treatment of the responders to initial gefitinib therapy was strongly dependent on EGFR-TKIs: almost half of the total treatment time was occupied by gefitinib therapy. Since the median time period occupied by gefitinib was 926 days in the 5-year survivors, gefitinib therapy was again an important factor in their long-term survival. Being *EGFR* mutation status as an exception, we could not find out the factors which were consistently different between overall patients and 3-, 4-, or 5-year survivors. We think that the difference in *EGFR* mutation status simply reflects the fact that the mutation analysis of *EGFR* became possible in 2007 and the patients who were diagnosed before 2007 usually received gefitinib without mutation data of *EGFR*.

Kaplan–Meier and multivariate analysis showed a significant reduction of HR by gefitinib rechallenge and a tendency of reduction by gefitinib BPD. However, these results should be carefully interpreted due to several biases. To better analyze the effect of these strategies, we adopted a DTRA. The DTRA suggested that the gefitinib rechallenge lengthened OS by an average of 46 days compared with therapy consisting of gefitinib followed only by cytotoxic drugs, although the difference was not statistically significant (Fig. 3). Recently, some reports have suggested that gefitinib BPD is also useful for patients who initially respond to gefitinib [11]. Additionally, Chaft et al. reported that discontinuation of an EGFR-TKI resulted in a rapid symptomatic progression and even disease flares in the patients with acquired resistance [16]. In our study, gefitinib BPD showed significant improvement of OS by Kaplan–Meier analysis, although the difference was not statistically significant by multivariate analysis. These results are not conclusive, but the studies in other types of cancer with an oncogenic driver mutation or a molecule essential for tumor growth support the effectiveness of continuing treatment BPD [17,18].

In the present study, we selected the responders to initial gefitinib treatment instead of the patients with NSCLC harboring activated *EGFR* mutations. Since the analysis of *EGFR* mutation became available in 2007, we considered that the latter way of patient selection decreased the study size resulting in poor statistical power. We defined the responders as CR, PR, or SD with duration of over 6 months in the protocol. This criterion was included in Jackman's criteria, which is known to define acquired resistance to an EGFR-TKI, clinically [19]. It is also reported that only 8% NSCLC with wild type *EGFR* met Jackman's criteria in landmark IPASS trial [20]. In contrast, EGFR-TKIs are not effective in 20–30% patients even if they carry NSCLC with activated EGFR. Gefitinib rechallenge and BPD will make sense only when they are applied to the responders to gefitinib.

The vast majority of patients that initially respond to an EGFR-TKI develop acquired resistance, and the mechanisms for this continue to be extensively studied. Various mechanisms of resistance have been reported, including secondary mutations in *EGFR* [21,22], *MET* amplification [23,24], *PTEN* down regulation [25,26], *CRKL* amplification [27], high-levels of HGF expression [28], FAS–NFκB pathway activation [29], epithelial–mesenchymal transition [30], and phenotypic conversion to small cell lung cancer [30,31], *etc.* Developing inhibitors that target these mechanisms is an important goal. The problem is more complicated however by the likely heterogeneous nature of EGFR-TKI resistant tumors. Using an animal model, Chmielecki et al. found that even if only 25% of cells in a tumor are resistant to an EGFR-TKI, whereas the entire tumor appears to acquire resistance [32]. Recent reports describing flare phenomenon after the cessation of EGFR-TKI treatment may support these observations [16,33]. If a tumor that acquired resistance to an EGFR-TKI actually consists of both sensitive and resistant clones, it would be reasonable to administer EGFR-TKIs beyond progression, as sensitive clones should still be targeted. Several phase II studies have incorporated this strategy, and their results seems to favor EGFR-TKI rechallenge and BPD [34–36]. However, the patient numbers in these studies were too small to determine the statistical significance.

The present study has a few limitations. Firstly, EGFR mutation status was unknown in more than half patients. However, focusing on the responder to initial gefitinib treatment is a possible way to evaluate the study objectives as described above. Second, this is a retrospective study, although it was performed based on a protocol. Third, it is difficult to analyze the effects of gefitinib rechallenge and BPD as completely separate entities as they are interrelated. It is clear that prospective randomized phase III studies are necessary to answer the clinical questions that we have addressed in this manuscript, and some studies are currently underway. The results of this study suggested that EGFR-TKI rechallenge and BPD played a central role to long-term survival of patients who initially responded to gefitinib.

Funding

This work was supported by an Investigator Sponsored Study Program of AstraZeneca Japan.

Conflicts of interest statement

K. Nishino has received honoraria from Chugai. F. Imamura has received honoraria from AstraZeneca, Ono and Chugai. S. Morita has received honoraria from AstraZeneca. T. Kijima has received honoraria from Chugai. All other authors have declared no conflicts of interest.

Acknowledgements

The authors thank all the participants of this study.

References

[1] Schiller JH, Harrington D, Belani CP, Langer C, Sandler A, Krook J, et al. Comparison of four chemotherapy regimens for advanced non-small-cell lung cancer. N Engl J Med 2002;346:92–8.

[2] Ohe Y, Ohashi Y, Kubota K, Tamura T, Nakagawa K, Negoro S, et al. Randomized phase III study of cisplatin plus irinotecan versus carboplatin plus paclitaxel, cisplatin plus gemcitabine, and cisplatin plus vinorelbine for advanced non-small-cell lung cancer: Four-Arm Cooperative Study in Japan. Ann Oncol 2007;18:317–23.

[3] Lynch TJ, Bell DW, Sordella R, Gurubhagavatula S, Okimoto RA, Brannigan BW, et al. Activating mutations in the epidermal growth factor receptor underlying responsiveness of non-small-cell lung cancer to gefitinib. N Engl J Med 2004;350:2129–39.

[4] Janne PA, Gurubhagavatula S, Yeap BY, Lucca J, Ostler P, Skarin AT, et al. Outcomes of patients with advanced non-small cell lung cancer treated with gefitinib (ZD1839, "Iressa") on an expanded access study. Lung Cancer 2004;44:221–30.

[5] Maemondo M, Inoue A, Kobayashi K, Sugawara S, Oizumi S, Isobe H, et al. Gefitinib or chemotherapy for non-small-cell lung cancer with mutated EGFR. N Engl J Med 2010;362:2380–8.

[6] Mitsudomi T, Morita S, Yatabe Y, Negoro S, Okamoto I, Tsurutani J, et al. Gefitinib versus cisplatin plus docetaxel in patients with non-small-cell lung cancer harbouring mutations of the epidermal growth factor receptor (WJTOG3405): an open label, randomised phase 3 trial. Lancet Oncol 2010;11:121–8.

[7] Morita S, Okamoto I, Kobayashi K, Yamazaki K, Asahina H, Inoue A, et al. Combined survival analysis of prospective clinical trials of gefitinib for non-small cell lung cancer with EGFR mutations. Clin Cancer Res 2009;15:4493–8.

[8] Zhou C, Wu YL, Chen G, Feng J, Liu XQ, Wang C, et al. Erlotinib versus chemotherapy as first-line treatment for patients with advanced EGFR mutation-positive non-small-cell lung cancer (OPTIMAL, CTONG-0802): a multicentre, open-label, randomised, phase 3 study. Lancet Oncol 2011;12:735–42.

[9] Rosell R, Carcereny E, Gervais R, Vergnenegre A, Massuti B, Felip E, et al. Erlotinib versus standard chemotherapy as first-line treatment for European patients with advanced EGFR mutation-positive non-small-cell lung cancer (EURTAC): a multicentre, open-label, randomised phase 3 trial. Lancet Oncol 2012;13:239–46.

[10] Watanabe S, Tanaka J, Ota T, Kondo R, Tanaka H, Kagamu H, et al. Clinical responses to EGFR-tyrosine kinase inhibitor retreatment in non-small cell lung cancer patients who benefited from prior effective gefitinib therapy: a retrospective analysis. BMC Cancer 2011;11:1.

[11] Nishie K, Kawaguchi T, Tamiya A, Mimori T, Takeuchi N, Matsuda Y, et al. Epidermal growth factor receptor tyrosine kinase inhibitors beyond progressive disease: a retrospective analysis for Japanese patients with activating EGFR mutations. J Thorac Oncol 2012;7:1722–7.

[12] Nishino M, Cardarella S, Dahlberg SE, Jackman DM, Ramaiya NH, Hatabu H, et al. Radiographic assessment and therapeutic decisions at RECIST progression in EGFR-mutant NSCLC treated with EGFR tyrosine kinase inhibitors. Lung Cancer 2013;79:283–8.

[13] Lunceford JK, Davidian M, Tsiatis AA. Estimation of survival distributions of treatment policies in two-stage randomization designs in clinical trials. Biometrics 2002;58:48–57.

[14] Wahed AS, Tsiatis AA. Optimal estimator for the survival distribution and related quantities for treatment policies in two-stage randomization designs in clinical trials. Biometrics 2004;60:124–33.

[15] Huang X, Cormier JN, Pisters PW. Estimation of the causal effects on survival of two-stage nonrandomized treatment sequences for recurrent diseases. Biometrics 2006;62:901–9.

[16] Chaft JE, Oxnard GR, Sima CS, Kris MG, Miller VA, Riely GJ. Disease flare after tyrosine kinase inhibitor discontinuation in patients with EGFR-mutant lung cancer and acquired resistance to erlotinib or gefitinib: implications for clinical trial design. Clin Cancer Res 2011;17:6298–303.

[17] Extra JM, Antoine EC, Vincent-Salomon A, Delozier T, Kerbrat P, Bethune-Volters A, et al. Efficacy of trastuzumab in routine clinical practice and after progression for metastatic breast cancer patients: the observational Hermine study. Oncologist 2010;15:799–809.

[18] Schnadig ID, Blanke CD. Gastrointestinal stromal tumors: imatinib and beyond. Curr Treat Opt Oncol 2006;7:427–37.

[19] Jackman D, Pao W, Riely GJ, Engelman JA, Kris MG, Janne PA, et al. Clinical definition of acquired resistance to epidermal growth factor receptor tyrosine kinase inhibitors in non-small-cell lung cancer. J Clin Oncol 2010;28:357–60.

[20] Mok TS, Wu YL, Thongprasert S, Yang CH, Chu DT, Saijo N, et al. Gefitinib or carboplatin–paclitaxel in pulmonary adenocarcinoma. N Engl J Med 2009;361:947–57.

[21] Kobayashi S, Boggon TJ, Dayaram T, Janne PA, Kocher O, Meyerson M, et al. EGFR mutation and resistance of non-small-cell lung cancer to gefitinib. N Engl J Med 2005;352:786–92.

[22] Pao W, Miller VA, Politi KA, Riely GJ, Somwar R, Zakowski MF, et al. Acquired resistance of lung adenocarcinomas to gefitinib or erlotinib is associated with a second mutation in the EGFR kinase domain. PLoS Med 2005;2:e73.

[23] Engelman JA, Zejnullahu K, Mitsudomi T, Song Y, Hyland C, Park JO, et al. MET amplification leads to gefitinib resistance in lung cancer by activating ERBB3 signaling. Science 2007;316:1039–43.

[24] Bean J, Brennan C, Shih JY, Riely G, Viale A, Wang L, et al. MET amplification occurs with or without T790M mutations in EGFR mutant lung tumors with acquired resistance to gefitinib or erlotinib. Proc Natl Acad Sci USA 2007;104:20932–7.

[25] Yamasaki F, Johansen MJ, Zhang D, Krishnamurthy S, Felix E, Bartholomeusz C, et al. Acquired resistance to erlotinib in A-431 epidermoid cancer cells requires down-regulation of MMAC1/PTEN and up-regulation of phosphorylated Akt. Cancer Res 2007;67:5779–88.

[26] Kokubo Y, Gemma A, Noro R, Seike M, Kataoka K, Matsuda K, et al. Reduction of PTEN protein and loss of epidermal growth factor receptor gene mutation in lung cancer with natural resistance to gefitinib (IRESSA). Br J Cancer 2005;92:1711–9.

[27] Cheung HW, Du J, Boehm JS, He F, Weir BA, Wang X, et al. Amplification of CRKL induces transformation and epidermal growth factor receptor inhibitor resistance in human non-small cell lung cancers. Cancer Discov 2011;1:608–25.

[28] Yano S, Yamada T, Takeuchi S, Tachibana K, Minami Y, Yatabe Y, et al. Hepatocyte growth factor expression in EGFR mutant lung cancer with intrinsic and acquired resistance to tyrosine kinase inhibitors in a Japanese cohort. J Thorac Oncol 2011;6:2011–7.

[29] Bivona TG, Hieronymus H, Parker J, Chang K, Taron M, Rosell R, et al. FAS and NF-kappaB signalling modulate dependence of lung cancers on mutant EGFR. Nature 2011;471:523–6.

[30] Sequist LV, Waltman BA, Dias-Santagata D, Digumarthy S, Turke AB, Fidias P, et al. Genotypic and histological evolution of lung cancers acquiring resistance to EGFR inhibitors. Sci Transl Med 2011;3:75ra26.

[31] Suda K, Mizuuchi H, Maehara Y, Mitsudomi T. Acquired resistance mechanisms to tyrosine kinase inhibitors in lung cancer with activating epidermal growth factor receptor mutation-diversity, ductility, and destiny. Cancer Metastasis Rev 2012;31:807–14.

[32] Chmielecki J, Foo J, Oxnard GR, Hutchinson K, Ohashi K, Somwar R, et al. Optimization of dosing for EGFR-mutant non-small cell lung cancer with evolutionary cancer modeling. Sci Transl Med 2011;3:90ra59.

[33] Riely GJ, Kris MG, Zhao B, Akhurst T, Milton DT, Moore E, et al. Prospective assessment of discontinuation and reinitiation of erlotinib or gefitinib in patients with acquired resistance to erlotinib or gefitinib followed by the addition of everolimus. Clin Cancer Res 2007;13:5150–5.

[34] Asahina H, Oizumi S, Inoue A, Kinoshita I, Ishida T, Fujita Y, et al. Phase II study of gefitinib readministration in patients with advanced non-small cell lung cancer and previous response to gefitinib. Oncology 2010;79:423–9.

[35] Oh IJ, Ban HJ, Kim KS, Kim YC. Retreatment of gefitinib in patients with non-small-cell lung cancer who previously controlled to gefitinib: a single-arm, open-label, phase II study. Lung Cancer 2012;77:121–7.

[36] Koizumi T, Agatsuma T, Ikegami K, Suzuki T, Kobayashi T, Kanda S, et al. Prospective study of gefitinib readministration after chemotherapy in patients with advanced non-small-cell lung cancer who previously responded to gefitinib. Clin Lung Cancer 2012;13:458–63.

FEBS Open Bio 3 (2013) 225–230

journal homepage: www.elsevier.com/locate/febsopenbio

Calretinin mediates apoptosis in small cell lung cancer cells expressing tetraspanin CD9☆

Ping He[a,c,1], Hanako Kuhara[a,1], Isao Tachibana[a,*], Yingji Jin[a], Yoshito Takeda[a], Satoshi Tetsumoto[a], Toshiyuki Minami[a], Satoshi Kohmo[a], Haruhiko Hirata[a], Ryo Takahashi[a], Koji Inoue[a], Izumi Nagatomo[a], Hiroshi Kida[a], Takashi Kijima[a], Tetsuji Naka[a,d], Eiichi Morii[b], Ichiro Kawase[a], Atsushi Kumanogoh[a,e]

[a] Department of Respiratory Medicine, Allergy and Rheumatic Diseases, Osaka University Graduate School of Medicine, Osaka 565-0871, Japan
[b] Department of Pathology, Osaka University Graduate School of Medicine, Osaka 565-0871, Japan
[c] Department of Respiratory Medicine, The Second Affiliated Hospital, School of Medicine, Xi'an Jiaotong University, Xi'an 71004, China
[d] Laboratory of Immune Signal, National Institute of Biomedical Innovation, Osaka 567-0085, Japan
[e] CREST, JST, Department of Immunopathology, WPI Immunology Frontier Research Center, Osaka University, Osaka 565-0871, Japan

ARTICLE INFO

Article history:
Received 17 January 2013
Received in revised form 5 April 2013
Accepted 26 April 2013

Keywords:
Small cell lung cancer
Proteomics
Tetraspanin
CD9
Calretinin
Apoptosis

ABSTRACT

A majority of small cell lung cancer (SCLC) cells lack a metastasis suppressor, tetraspanin CD9, and CD9 expression promotes their apoptosis. By a proteomics-based approach, we compared an SCLC cell line with its CD9 transfectant and found that a calcium-binding neuronal protein, calretinin, is upregulated in CD9-positive SCLC cells. Ectopic or anticancer drug-induced CD9 expression upregulated calretinin, whereas CD9 knockdown down-regulated calretinin in SCLC cells. When calretinin was knocked down, CD9-positive SCLC cells revealed increased Akt phosphorylation and decreased apoptosis. These results suggest that CD9 positively regulates the expression of calretinin that mediates proapoptotic effect in SCLC cells.

1. Introduction

Small cell lung cancer (SCLC) is highly malignant lung tumor that spreads early throughout the body. It is characterized by neuroendocrine features such as neuropeptide production and N-CAM expression [1]. At diagnosis in most cases, SCLC has already metastasized to regional lymph nodes and distant organs including brain, bone, liver, and adrenal gland, thus excluding the possibility of surgical resection. Currently, standard treatment against extended SCLC is chemotherapy including cisplatin and etoposide [2]. Despite its high sensitivity to these anticancer drugs, SCLC rapidly develops recurrent tumors locally and at the distant organs. Such malignant phenotype is at least partially caused by acquired resistance to apoptotic cell death [3]. Elucidation of its mechanisms is necessary to improve outcome of chemotherapy, but little has been clarified.

Tetraspanins are a family of membranous proteins that has characteristic structure spanning the membrane four times. Through association with other functional proteins including integrins, growth factor receptors, membrane proteases, and intracellular signaling molecules, tetraspanins organize multiprotein complexes at the tetraspanin-enriched microdomain (TEM) and regulate cell adhesion, migration, and survival [4,5]. Among 33 members in humans, CD9 and CD82 are known as a metastasis suppressor of solid tumors. Clinical and pathological findings suggest that decreased expressions of these tetraspanins are associated with progression of cancers of breast, pancreas, colon, and esophagus, and nonsmall cell lung cancer (NSCLC) and thus with poor prognosis [6,7].

We have shown that, among tetraspanins, CD9 is selectively absent in a majority of SCLC lines and SCLC tissues in contrast to NSCLC which frequently expresses CD9, and that ectopic expression of CD9 in SCLC cells suppresses integrin β1-dependent cell motility [8] and promotes apoptotic cell death through attenuation of PI3K/Akt signaling [9]. These results suggest that the absence of CD9 contributes to highly malignant phenotype of SCLC. We also found that CD9 expression is induced and cell motility is decreased when SCLC cells are exposed to cisplatin or etoposide [10]. In the present study, we compared an SCLC cell line with its CD9 transfectant by a proteomics-based approach and found that a calcium-binding neuronal protein,

Abbreviations: SCLC, small cell lung cancer; NSCLC, nonsmall cell lung cancer; PARP, poly(ADP-ribose)polymerase; PMF, peptide mass fingerprinting; MALDI-TOF, matrix-assisted laser desorption/ionization time-of-flight; RT-PCR, reverse transcription-PCR; KO, knockout

[1] These authors contributed equally to the study.

* Corresponding author. Tel.: +81 6 6879 3833; fax: +81 6 6879 3839.
E-mail address: itachi02@imed3.med.osaka-u.ac.jp (I. Tachibana).

2211-5463/$36.00
http://dx.doi.org/10.1016/j.fob.2013.04.005

calretinin, is upregulated in CD9-positive SCLC cells. We also show that calretinin mediates apoptotic cell death of SCLC.

2. Materials and methods

2.1. Cell lines

OS1, OS2-RA, and OS3-R5 were SCLC cell lines established in our laboratory, and their biological properties were previously characterized [8]. SCLC lines, OC10 and CADO LC6, a lung adenocarcinoma cell line, CADO LC9, and a mesothelioma cell line, OC-(MT)37, were provided by Osaka Medical Center for Cancer and Cardiovascular Diseases (Osaka, Japan) [11]. An SCLC line, SBC-3, and its chemoresistant subline, SBC-3/CDDP, were kindly provided by Dr. K. Kiura (Okayama University, Okayama, Japan) [10]. SCLC cell lines, NCI-H69, NCI-N231, and NCI-H209, a lung adenocarcinoma line, A549, and pleural mesothelioma lines, NCI-H226, NCI-H2452, NCI-H28, and MSTO-211H, were purchased from American Type Culture Collection (Rockville, MD). A lung squamous cell carcinoma line, HARA, was a kind gift from Dr. H. Iguchi (Kyusyu Cancer Center, Fukuoka, Japan). All cell lines were maintained in RPMI 1640 medium supplemented with 10% heat-inactivated FBS, 100 U/ml penicillin, and 100 μg/ml streptomycin.

2.2. Antibodies and reagents

Mouse anti-CD9 mAb (MM2/57), anti-poly(ADP-ribose)polymerase (PARP) mAb (42/PARP), and anti-β-actin mAb (C4) were purchased from Biosource, BD Biosciences, and Santa Cruz Biotechnology, respectively. Mouse anti-CD9 mAb (72F6) was purchased from Novocastra. Goat anti-calretinin polyclonal Ab (AB1550) and rabbit anti-calretinin polyclonal Ab (DC8) were purchased from Chemicon International and Zymed Laboratories, respectively. Rabbit anti-cleaved PARP (Asp214) mAb (D64E10), anti-phospho-Akt (Ser473) mAb (D9E), and anti-Akt polyclonal Ab were purchased from Cell Signaling Technology. Cisplatin (CDDP) was provided by Nippon Kayaku Co. (Tokyo, Japan).

2.3. Flow cytometry

Cells (10^4) were incubated with 10 μg/ml primary mouse mAbs and labeled with FITC-conjugated goat anti-mouse immunoglobulin (Biosourece International). Normal mouse IgG was used as a control. Stained cells were analyzed on a FACScan (Becton Dickinson).

2.4. cDNA and small interfering RNA (siRNA) transfection

Establishment of stable CD9-, NAG-2-, and mock-transfectants of OS3-R5 was previously described [8,9]. Cells were transfected with 40 nM cocktail siRNAs against human CD9 (No. SHF27A-0631; B-Bridge International) or human calretinin (No. SHF27A-0981; B-Bridge International), or negative control cocktail RNAs (No. S30C-0126; B-Bridge International) using LipofectAMINE 2000 Reagent (Invitrogen).

2.5. Two-dimensional electrophoresis (2-DE) and mass spectrometry analysis

Proteins were extracted from cells with the Complete Mammalian Proteome Extraction Kit (Calbiochem, Darmstadt, Germany). For 2-DE, isoelectric focusing (IEF) was performed using the PROTEAN IEF cell (Bio-Rad laboratories) according to the manufacturer's instructions. Extracted proteins were reconstituted in a rehydration buffer (7 M urea, 2 M thiourea, 4% CHAPS, 2 mM tributylphosphine (TBP), 0.0002% bromophenol blue (BPB), 0.2% Bio-lyte ampholyte 4–7) and applied to ReadyStrip™ IPG strips (11 cm, pH 4–7). IEF was run for 45,000 Vh. Two-dimensional electrophoresis was carried out in 10% Bis–Tris Criterion™ XT Precast gels. After staining with the Silver Stain MS Kit (Wako Pure Chemical Industries, Osaka, Japan), the gels were captured by transmission scanning and analyzed with Image Master 5.0 (Amersham Biosciences). Following analysis, selected protein spots were manually excised from the gels and digested with trypsin (Promega) according to published procedures [12]. All peptide mass fingerprinting (PMF) spectra were obtained by using an ultraflex TOF/TOF matrix-assisted laser desorption/ionization time-of-flight (MALDI-TOF) mass spectrometer (Bruker Daltonics, Bremen, Germany).

2.6. Database search

PMF data were searched with Mascot software (Matrix Science, London, UK) against NCBInr or Swiss-Prot databases. Protein database searching was performed with following parameters: *Homo sapiens*, maximum of one missed, cleavage by trypsin, monoisotopic masse value, charge state of 1 +, allowing a mass tolerance of 100 ppm, and carbamidomethyl modification of cysteine. Protein scores of >64 indicate identity or extensive homology ($P < 0.05$) and were considered significant.

2.7. Reverse transcription-PCR (RT-PCR)

One microgram of total RNA was reversely transcribed with a cDNA synthesis kit (Invitrogen) using random hexamers. The thermal cycling parameters were 30 cycles of 40 s at 94 °C, 40 s at 60 °C, and 90 s at 72 °C for CD9 and 30 cycles of 30 s at 94 °C, 30 s at 60 °C, and 90 s at 72 °C for calretinin. We confirmed that these variables yielded amplification of template DNAs within a linear range. The sequences of upstream and downstream oligonucleotide primers for CD9 was previously described [8]. Upstream and downstream oligonucleotide primers used for calretinin were 5′-GGAAGCACTTTGACGCAGACG-3′ and 5′-CTCGCTGCAGAGCACAATCTC-3′, respectively.

2.8. Immunoprecipitation and immunoblotting

Cells were lysed in lysis buffer containing 1% Brij 99, 25 mM HEPES, pH 7.5, 150 mM NaCl, 5 mM $MgCl_2$, 2 mM phenylmethylsulfonyl fluoride, 10 μg/ml aprotinin, and 10 μg/ml leupeptin. Whole cell lysates or immunoprecipitates with anti-CD9 mAb (MM2/57) were separated by 10% SDS-PAGE under nonreducing conditions for CD9 or under reducing conditions for the other proteins. After transfer to Immobilon-P membranes (Millipore), immunoblotting was performed with primary Abs followed by peroxidase-conjugated secondary Abs. Immunoreactive bands were visualized with a chemiluminescent reagent (PerkinElmer).

2.9. Immunohistochemistry

A human SCLC tissue array was purchased from US Biomax Inc. It contained small cell carcinoma tissues from 30 individuals and normal tissues from three individuals. Each specimen was represented by two cores from different tissue spots. After antigen retrieval, inactivation of endogenous peroxidase, and blockade of non-specific reaction, the tissue microarray sections were stained with anti-CD9 mAb (72F6) or anti-calretinin Ab (DC8), followed by incubation with biotinylated goat anti-mouse and rabbit IgG Ab and streptavidin-conjugated peroxidase. These were counterstained with Mayer's hematoxylin [10]. Specimens were regarded as positive when staining was observed in more than 30% of tumor cells on average. The significance of association between CD9 staining and calretinin staining was evaluated by Fisher's exact test.

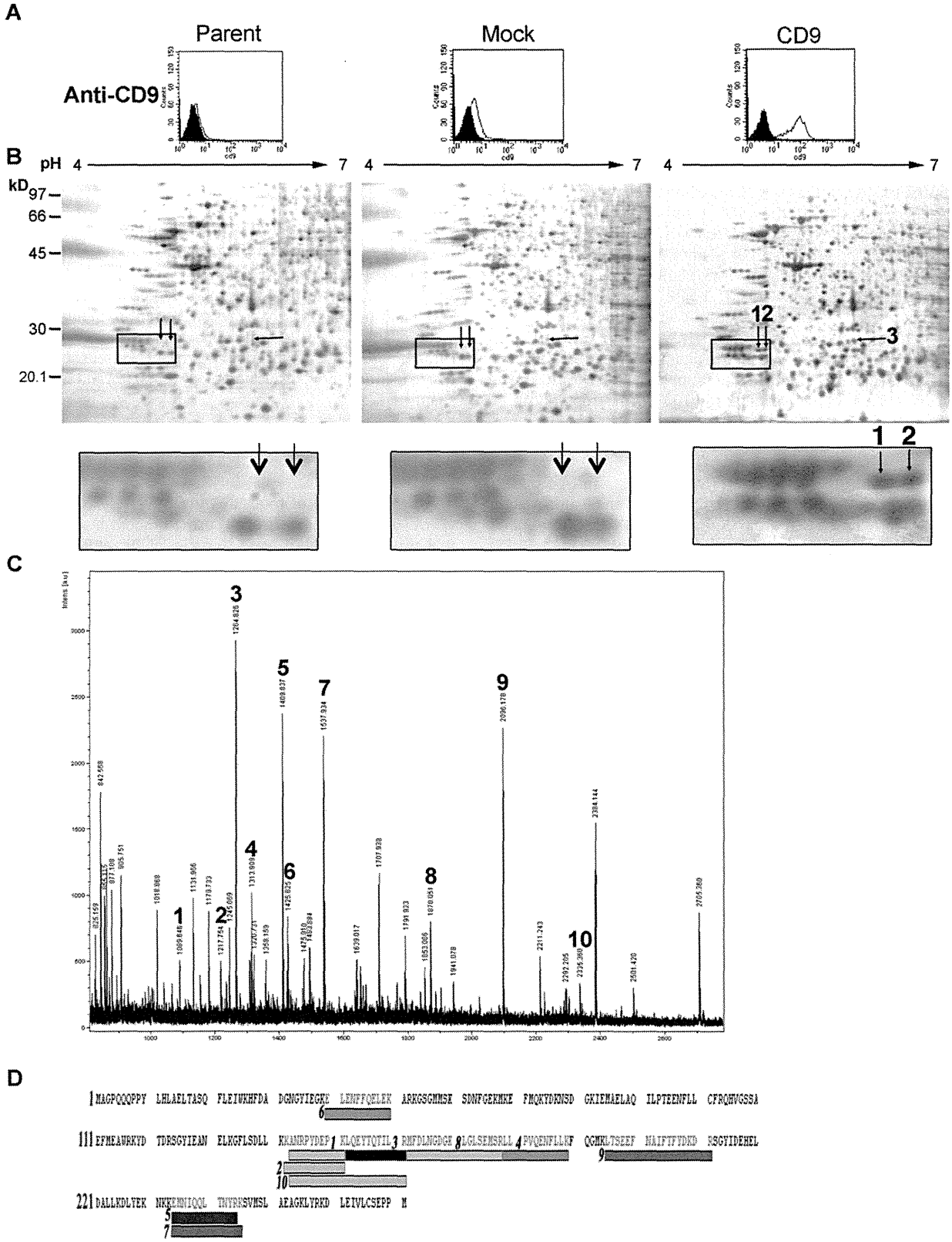

Fig. 1. Comparative proteomic analysis of the parent and CD9-overexpressing SCLC cells. (A) The parent, mock transfectant, and CD9 transfectant of OS3-R5 were stained with anti-CD9 mAb, labeled with FITC-conjugated goat anti-mouse immunoglobulin, and analyzed on a FACScan (*Open histograms*). *Closed histograms* indicate staining with control IgG. (B) Representative 2-DE maps of OS3-R5 and its transfectants. *Arrows* 1–3 indicate protein spots selectively identified in OS3-R5-CD9 by mass spectrometry. 1 and 2, calretinin; 3, PA28α. Images including the calretinin spots were enlarged in *lower columns*. (C) PMF spectra of spot 2 obtained by MALDI-TOF. Mass peaks, peptides of which were matched with human calretinin, are marked with numbers. (D) The matched peptides in panel (C) were indicated with bars, yielding 33% sequence coverage of calretinin.